NUMERICAL INVESTIGATION ON EFFECTS OF PLAIN, PERFORATED, AND DIMPLED TWISTED TAPE INSERTS IN A TUBE TO FLOW AND HEAT TRANSFER CHARACTERISTICS

2023
MASTER THESIS
MECHANICAL ENGINEERING

Omar Wageeh Abass ABASS

Thesis Advisor
Assist. Prof. Dr. Mutlu TEKİR

NUMERICAL INVESTIGATION ON EFFECTS OF PLAIN, PERFORATED, AND DIMPLED TWISTED TAPE INSERTS IN A TUBE TO FLOW AND HEAT TRANSFER CHARACTERISTICS

Omar Wageeh Abass ABASS

Thesis Advisor

Assist. Prof. Dr. Mutlu TEKİR

T.C.

Karabuk University

Institute of Graduate Programs

Department of Mechanical Engineering

Prepared as

Master Thesis

KARABUK

August 2023

I certify that in my opinion the thesis submitted by Omar Wageeh Abass ABASS titled "NUMERICAL INVESTIGATION ON EFFECTS OF PLAIN, PERFORATED, AND DIMPLED TWISTED TAPE INSERTS IN A TUBE TO FLOW AND HEAT TRANSFER CHARACTERISTICS" is fully adequate in scope and in quality as a thesis for the degree of Master of Science.

Assist. Prof. Dr. Mutlu TEKİR .....

Thesis Advisor, Department of Mechanical Engineering

This thesis is accepted by the examining committee with a unanimous vote in the Department of Mechanical Engineering as a Master of Science thesis. August 22, 2023

Examining Committee Members (Institutions)	Signature
Chairman : Assist. Prof. Dr. Mehmet GÜRDAL (KÜ)	.....
Member : Prof. Dr. Kamil ARSLAN (KBÜ)	.....
Member : Assist. Prof. Dr. Mutlu TEKİR (KBÜ)	.....

The degree of Master of Science by the thesis submitted is approved by the Administrative Board of the Institute of Graduate Programs, Karabuk University.

Assoc. Prof. Dr. Zeynep ÖZCAN .....

Director of the Institute of Graduate Programs

"I declare that all the information within this thesis has been gathered and presented in accordance with academic regulations and ethical principles and I have according to the requirements of these regulations and principles cited all those which do not originate in this work as well."

Omar Wageeh Abass ABASS

ABSTRACT

M. Sc. Thesis

NUMERICAL INVESTIGATION ON EFFECTS OF PLAIN, PERFORATED, AND DIMPLED TWISTED TAPE INSERTS IN A TUBE TO FLOW AND HEAT TRANSFER

Omar Wageeh Abass ABASS

Karabuk University
Institute of Graduate Programs
The Department of Mechanical Engineering

Thesis Advisor:
Assist. Prof. Dr. Mutlu TEKİR
August 2023, 72 pages

This research delves into improving heat transfer within a tube by incorporating twisted tape inserts. The study employs a numerical approach to solve the governing equations, which include the continuity equation, momentum equation, and energy equation. The investigation comprises seven distinct cases aimed at augmenting heat transfer: a basic twisted tape, a perforated twisted tape with lengths of 25 mm, 50 mm, and 100 mm, as well as a dimpled twisted tape with lengths of 25 mm, 50 mm, and 100 mm.

For each of these seven cases, we conducted analyses at five different Reynolds numbers (10,000, 12,000, 15,000, 18,000, and 20,000). The physical dimensions of the geometry include a tube length of 1000mm, an inner diameter of 17mm, and an outer diameter of 21mm. The twisted tape itself is also 1000mm long, with a width of

17mm and a thickness of 1mm. The water is a working fluid used in the study, and grid independent mesh was 532000, with Tetrahedral cells.

The results from the seven studied cases were compared to the original condition (smooth tube) in terms of Nusselt values and friction factor, and performance evaluation criteria were established. The best improvement was obtained for 25 mm dimpled twisted tape with 42%, while the improvement for perforated tape was 28.7% and for the plain tape was 24%. The higher value of fraction factors was obtained at 25 mm dimpled twisted tape.

Key Words : Twisted tape, heat transfer, CFD, plain, dimpled, perforated, performance evaluation criteria, heat exchanger tube, Nusselt number, friction factor.

Science Code : 91412

ÖZET

Yüksek Lisans Tezi

BİR TÜP İÇİNDEKİ DÜZ, DELİKLİ VE ÇUKUR KANATÇIKLI BURULMUŞ ŞERİTLERİN AKIŞ VE ISI TRANSFERİ ÜZERİNDEKİ ETKİSİNİN SAYISAL İNCELENMESİ

Omar Wageeh Abass ABASS

Karabük Üniversitesi
Lisansüstü Eğitim Enstitüsü
Makine Mühendisliği Anabilim Dalı

Tez Danışmanı:
Dr. Öğr. Üyesi Mutlu TEKİR
Ağustos 2023, 72 sayfa

Bu çalışmada, bükümlü bant ara parçaları bulunan bir borunun ısı transferinin arttırılması, ilgili denklemlerin (süreklilik denklemi, momentum denklemi ve enerji denklemi) sayısal bir yöntem kullanılarak çözülmesi araştırılmıştır. Isı transferini geliştirmek için yedi farklı durum çalışılmıştır: düz bükümlü bant, 25 mm, 50 mm ve 100 mm uzunluğunda delikli bükümlü bant ve 25 mm, 50 mm ve 100 mm uzunluğunda çukurlu bükümlü bant.

Bu yedi vakanın her biri için beş farklı Reynolds sayısında (10.000, 12.000, 15.000, 18.000 ve 20.000) analizler gerçekleştirdik. Geometrinin fiziksel boyutları 1000 mm'lik bir tüp uzunluğunu, 17 mm'lik bir iç çapı ve 21 mm'lik bir dış çapı içerir. Bükülmüş bandın kendisi de 1000 mm uzunluğunda, 17 mm genişliğinde ve 1 mm

kalınlığındadır. Su, çalışmada kullanılan bir çalışma sıvısıdır ve ızgaradan bağımsız ağ, tetrahedral hücreli 532000'dir.

İncelenen yedi vakadan elde edilen sonuçlar Nusselt değerleri ve sürtünme faktörü açısından orijinal durumla (düz boru) karşılaştırıldı ve performans değerlendirme kriterleri oluşturuldu. En iyi gelişme, %42 ile 25 mm çukurlu bükümlü bant elde edilirken, delikli bükümlü bantlarda %28,7 ve düz bantta %24 elde edildi. Ve 25 mm çukurlu bükümlü bantta kesir faktörlerinin değeri daha yüksektir.

Anahtar Kelimeler : Bükümlü bant, ısı transferi, CFD, düz, çukurlu, delikli, performans değerlendirme kriterleri, ısı değiştirici borusu, Nusselt sayısı, sürtünme faktörü

Bilim Kodu **:** 91412

ACKNOWLEDGMENTS

I would like to express my deep gratitude to my advisor and supervisor, Assist. Prof. Dr. Mutlu TEKİR, for the invaluable information, guidance, and unwavering support he has provided. Also, I would like to thank Prof. Dr. Kamil ARSLAN. His understanding and boundless kindness have meant a great deal to me. I am truly fortunate to have had the privilege of knowing them. I would also like to extend my heartfelt thanks to my family, particularly my mother, whose unwavering support has been my constant companion. Her assistance has been pivotal in my journey, and without her, I would be incomplete, unable to achieve anything. Therefore, this achievement is dedicated to you, my dear and wonderful mother.

Lastly, I am grateful to my friend Mohammed ALAMIRY for his continuous assistance. I must also express my appreciation to the other professors who have guided me along the right path.

TABLE OF CONTENTS

Page

Page

LIST OF FIGURES

Page

Page

LIST OF TABLES

Page

SYMBOLS AND ABBREVIATIONS INDEX

SYMBOLS

A_C : Cross section area (m^2)

C_p : Specific heat transfer ($J \cdot K^{-1} \cdot kg^{-1}$)

C_R : Coil ratio

D : The hydraulic diameter of pipe (m)

D_i : Inside diameter (m)

D_o : Outer diameter (m)

f : Friction factor of the induced tube

f_D : Gravitational constant (m/sec^2)

f_p : Friction factor of the induced plain tube

H : Pitch of twisted tape (mm)

h : Convective heat transfer coefficient ($W/m^2.K$)

j : Amount of radiation (W/m^2)

K : Thermal conductivity of the fluid (W/m.K)

L : Length of the tube (m)

M : Mass flow (kg)

Nu_p : Nusselt number of the induced plain tube.

Nu : Nusselt number

P : Pitch of twisted tape (mm)

P_c : Pitch of wire coil (mm)

P_d : Dimple twisted tape pitch (mm)

P_P : Perforated twisted tape pitch (mm)

Pr : Prandtl number

P_R : Pitch ratio

P_t : Pitch of twisted tape (mm)

P_1 : Pitch length of large twisted tape (mm)

P_2 : Pitch length of small twisted tape (mm)

Q : Local heat flux density (W/m^2)

Re : Reynolds number

R_p : Porosity dimension

Saf : Average friction entropy generation rate (J/K)

Sah : Average heat transfer entropy generation rate (J/K)

ST : Straight U tube without twisted tape (m)

t : Time (s)

U : Velocity in x- axis (m/s)

v : Velocity of the fluid (m/s)

V : Velocity in y- axis (m/s)

V_m : Mean velocity (m/s)

W : Width of twisted (mm)

w : Velocity in z- axis (m/s)

y : Twist ratio

Δh : The head loss due to friction (m)

ΔP : Pressure drop (Pa)

ΔT : Change of temperature (K)

ρ : Density of the fluid ($kg \cdot m^{-3}$)

μ : Dynamic viscosity ($kg \cdot m^{-1} \cdot s^{-1}$)

σ : Boltzmann constant ($5.67 \cdot 10^{-8}$)

ŋ : Thermal performance factor

Ø : Dissipation function

ABBREVIATIONS

ACT : Annularly corrugated twist.

ACTT : Alternate circular twisted tapes.

CTT : Classical twisted tapes.

DCTT : Double cut twisted tapes.

DDPT : Dense dimpled protruded twisted tape.

DDT : Dense dimple twisted tapes.

DPT : Dimple protrusion twisted tapes.

DTTE : Dimpled twisted tape edge inserted tube.

DTT : Dimple twisted tapes.

FLTT : Full length twisted tapes.

HLDTT : Half-length downstream twisted tapes.

HLUTT : Half-length up stream twisted tapes.

ITTT : Increased tapered twisted tapes.

MTT : Modified twisted tapes.

PEC : Performance evaluation criteria.

PCTT : Parabolic cut twisted tapes.

PTTE : Perforated twisted tape edge inserted tube.

PTT : Plain twisted tapes.

PTTT : Perforated triple twisted tapes.

PT : Plain tube.

RCT : Rectangular cut twisted.

RTT : Road twisted tapes.

SGT : Spiral grooved tube.

STT : Solid twisted tapes.

TEE : Thermal enhancement efficiency.

TKE : Turbulent kinetic energy.

TOTT-CL\S : Twin over twisted tape in counter large / small combination.

TT : Twisted tapes.

VCTT : V – cut twisted tapes.

PART 1

INTRODUCTION

Heat transfer is a fundamental concept that permeates every aspect of our lives, influencing the behavior of matter and shaping the environment around us. At its core, heat transfer encompasses the mechanisms by which thermal energy moves from one object or substance to another due to a difference in temperature. This essential process is omnipresent, governing the comfort of our homes, the operation of complex industrial systems, the natural phenomena in our environment, and the functionality of countless technological innovations.

Understanding heat transfer is crucial for engineers, scientists, and designers across various disciplines, as it forms the backbone of many critical fields, including thermodynamics, fluid dynamics, materials science, and energy systems. The ability to control and optimize heat transfer is essential for improving the efficiency of energy conversion, designing effective cooling and heating systems, ensuring the safety of machinery, and developing innovative technologies that drive progress. From the design of advanced electronics to the analysis of climate patterns, heat transfer is an ever-present force, shaping the way we interact with our environment and paving the way for a more sustainable and technologically advanced future. We will delve into the fundamental modes of heat transfer—conduction, convection, and radiation—examining their principles, real-world applications, and the synergies that often arise when they intersect.

1.1. HEAT TRANSFER TYPES

1.1.1. Conduction Heat Transfer

Conduction is the mode of heat transfer that occurs in solid materials or between objects in direct physical contact. In this process, heat energy is transferred through

molecular interactions within a material. Vibrating particles in a hot region pass on their kinetic energy to neighboring particles with lower energy, causing them to vibrate more vigorously and thereby transmitting heat. Metals, for instance, are excellent conductors due to the mobility of their electrons, which allows heat to propagate rapidly through the material. Conversely, insulating materials have fewer free electrons and exhibit poor heat-conducting properties.

1.1.2. Convection heat transfer

Convection involves the transfer of heat through the motion of a fluid (liquid or gas). This mode of heat transfer is primarily driven by the movement of the fluid itself. When a fluid is heated, it becomes less dense and tends to rise, creating upward currents. Conversely, in cooler regions, the fluid becomes denser and sinks, creating downward currents. Convection can be natural (e.g., the rising of warm air above a heater) or forced (e.g., using a fan to circulate air in a room or employing pumps in a liquid cooling system). It plays a crucial role in heat exchange processes, such as in radiators, industrial ovens, and even atmospheric phenomena like ocean currents and weather patterns.

1.1.3. Radiation heat transfer

Radiation is the mode of heat transfer that doesn't require a medium or physical contact. It is the transfer of energy through electromagnetic waves, including infrared radiation. All objects with a temperature above absolute zero emit thermal radiation. This phenomenon is a fundamental part of everyday life, from feeling the warmth of the sun to observing the glow of a hot iron or a fire. Surfaces that absorb radiation also emit it, following the principles of blackbody radiation. A key aspect of radiation is that it can occur in a vacuum, making it essential for space applications and a critical factor in the Earth's energy balance.

Understanding these modes of heat transfer is essential for engineers, scientists, and designers, as it forms the basis for optimizing energy efficiency, designing effective heating and cooling systems, and tackling complex challenges in fields such as

materials science, HVAC (Heating, Ventilation, and Air Conditioning), thermal management in electronics, and even space exploration. Each mode has its unique characteristics and applications, and the synergy between them often plays a significant role in real-world scenarios.

1.2. METHODS OF HEAT TRANSFER ENHANCEMENT

Enhancing heat transfer is a critical field of research focused on enhancing the efficiency and efficacy of heat exchange procedures. Heat exchangers find extensive use in various sectors like industrial air conditioning and power generation plants. This extensive use has led to substantial energy consumption and contributed to global warming. The primary objective of augmenting heat transfer is to achieve a more streamlined heat exchanger by minimizing expenses, dimensions, and weight [1]. There are three approaches to enhance heat transfer: passive, active, and a combination of both.

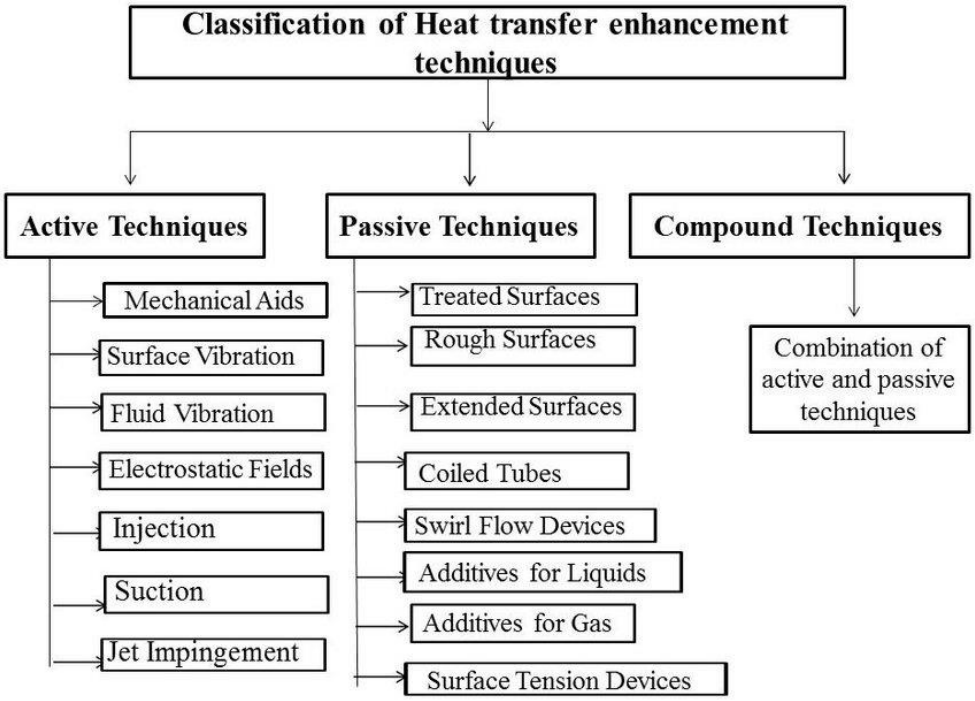

Figure 1.1. Classification of heat transfer enhancement techniques [2].

1.2.1. Passive method

Passive heat transfer enhancement refers to the utilization of inherently designed methods and natural phenomena to augment the efficiency of heat exchange processes without the need for external energy input or active control systems. This approach leverages fluid dynamics, surface modifications, geometrical configurations, or other passive mechanisms to optimize heat transfer rates, making it a sustainable and cost-effective solution. Passive methods are particularly advantageous in scenarios where simplicity, reliability, and reduced operational complexity are essential. By capitalizing on the innate properties of materials, fluids, or surface geometries, passive heat transfer enhancement techniques enhance thermal performance, leading to improved system efficiency, energy conservation, and more effective thermal management in various engineering applications.

Twisted tapes are recognized as a cost-effective and straightforward passive method for boosting heat transfer. They work by elevating the liquid's turbulence within the tube through the generation of vortices. Adjusting various parameters like the tape's shape, pitch, thickness, width, and twist ratio can further optimize heat transfer. Additionally, modifications such as incorporating holes or altering the tape's geometry can enhance its effectiveness [3]. When inserted inside a heat exchanger tube, twisted tapes create vortices, leading to improved liquid mixing driven by centrifugal force and vortex formation. This extended flow path ultimately enhances heat transfer [4]. They have found widespread application in heat exchanger tubes, where they induce turbulence near the tube wall and prolong the fluid's residence time within the tube [5]. Twisted tapes stand out as highly promising tools for generating swirl in the passive approach to enhancing heat transfer. They elevate heat transfer rates with only a minor increase in pressure loss, resulting in an overall enhancement of the system's thermal performance. However, it's worth noting that tubes with twisted tape inserts do experience higher frictional losses compared to those without inserts. Consequently, this increase in pressure drop can restrict the improvement in thermal performance.

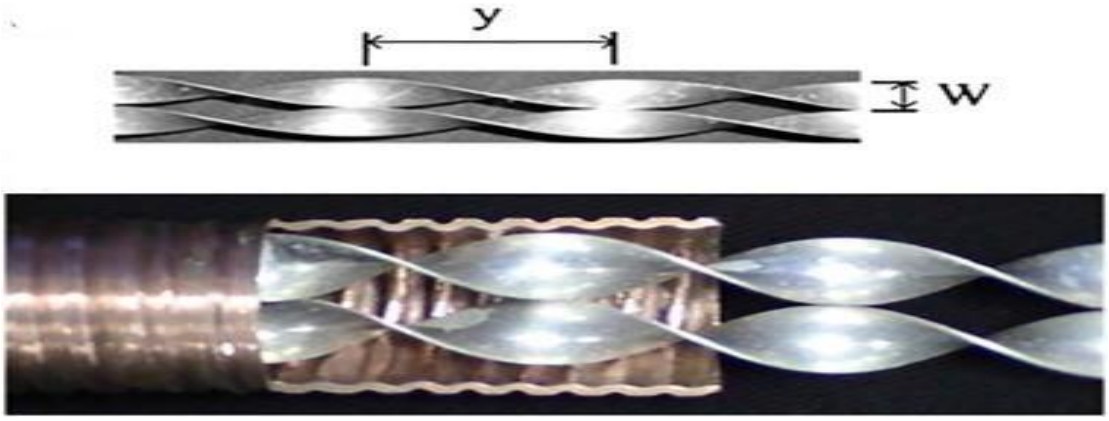

Figure 1.2. Twisted tapes inside a heat exchanger (passive method) [6].

1.2.2. Active Method

Active heat transfer enhancement refers to the deliberate application of external energy, control systems, or mechanical means to boost the rate of heat exchange between fluids or materials in a system. This approach involves the use of devices such as fans, pumps, heat exchanger configurations, or complex flow control mechanisms to increase the effectiveness of heat transfer processes. Active methods allow for fine-tuned control over heat transfer rates, enabling engineers and designers to optimize performance based on specific requirements. While active techniques can be highly effective in achieving rapid and precise heat transfer, they often come with increased operational complexity, energy consumption, and additional system components. These methods find applications in scenarios where immediate and controllable enhancement of heat exchange is necessary, albeit at the expense of increased energy usage and potential system complexity. An electric an injection, or magnetic field, fluid vibration, mechanical assistance, jet impingement, surface vibration, suction, etc. can be given as examples for this type of heat transfer enhancement method.

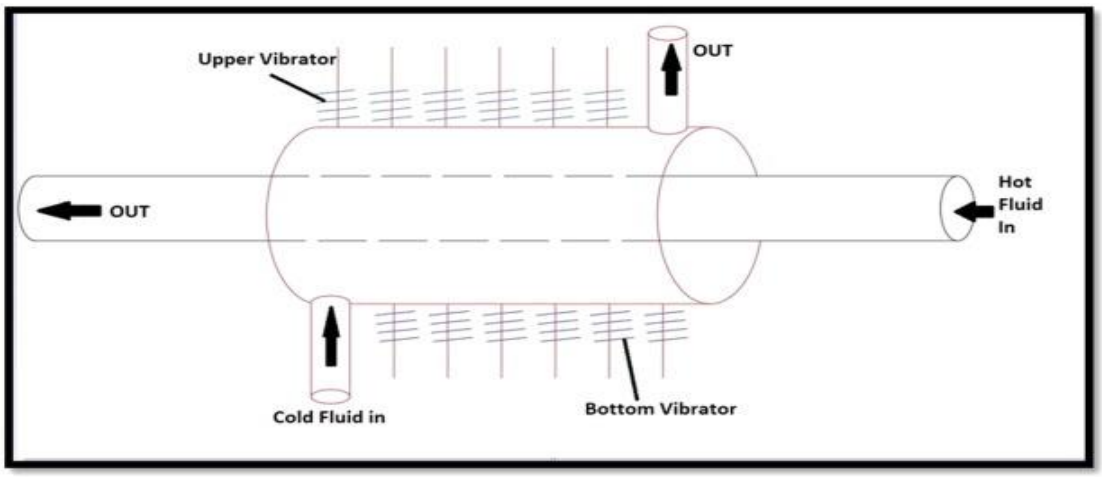

Figure 1.3. Heat exchanger (active method) [7].

1.2.3. Combined Method

Combined heat transfer enhancement refers to a comprehensive approach that synergistically combines both passive and active methods to optimize heat exchange within a system. By integrating the strengths of both approaches, this method aims to achieve a balanced and efficient heat transfer enhancement solution. Passive techniques, leveraging natural phenomena and surface modifications, offer long-term sustainability and reduced complexity. Meanwhile, active methods, utilizing external energy input and control systems, provide fine-tuned and immediate heat transfer enhancements when needed. By carefully selecting and integrating these techniques, engineers can tailor the heat transfer enhancement to meet specific performance goals, energy efficiency targets, and operational requirements. This combined approach often results in improved overall system performance, offering the advantages of active control with the reliability and simplicity of passive strategies, thereby providing a versatile and adaptable solution for a wide range of engineering applications.

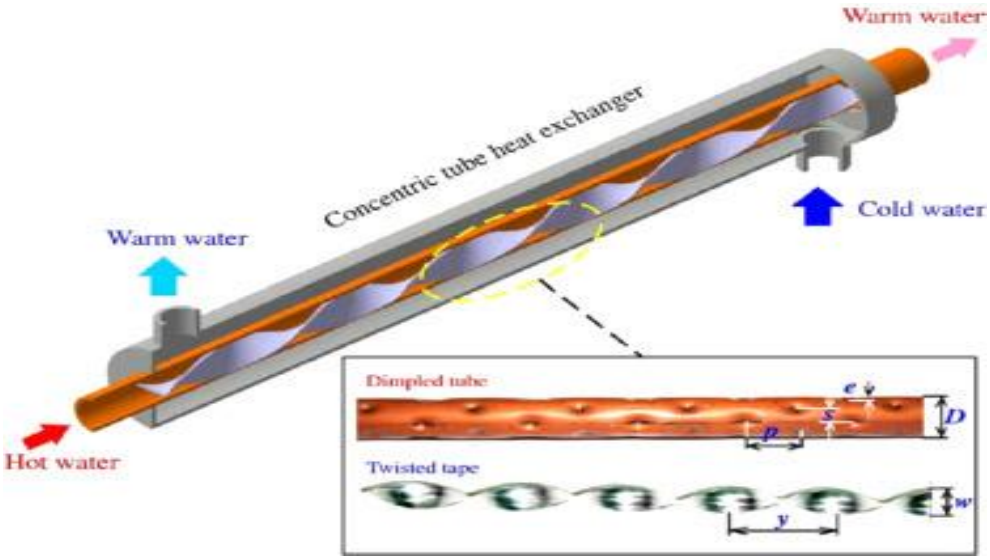

Figure 1.4. Twisted tapes inside heat exchanger (compound method) [6].

1.3. PERFORMANCE EVALUATION CRITERIA

This metric, referred to as the heat transfer enhancement index, is a widely recognized tool for assessing the real-world effectiveness of twisted tape. It provides empirical support for the practical viability of using twisted tape to enhance heat transfer. A parallel is drawn between the twisted tape insert within the tube and the smooth tube, assuming equal energy expenditure for tubes with or without the tape. This outcome is attained by factoring in both the improvements in heat transfer and the rise in pressure drop, and can be computed through mathematical formulas [8,9].

$$PEC = \frac{\left({Nu_p}/{Nu_s}\right)}{\left({f_p}/{f_s}\right)^{0.333}} \tag{1.1}$$

the Nusselt coefficients for the unadorned spiral (Nu_p), the Nusselt coefficients for the sleek cylinder (Nu_s), the resistance factor of the unadorned spiral (f_p), and the resistance factor of the sleek cylinder (f_s).

PART 2

LITERATURE REVIEW

In this section, a team of scientists sought to improve the heat transfer capabilities of a heat exchanger tube by employing a range of twisted tape variants. The selection of these tapes was based on their cost-effectiveness, ease of installation, minimal upkeep needs, and their effectiveness in enhancing heat transfer. The researchers conducted multiple adaptations to these tapes in order to attain optimal heat transfer outcomes. This included alterations in tape dimensions, spacing, the incorporation of surface irregularities, and experimenting with various shapes (either rectangular or square). Moreover, the team examined different liquid combinations, both with and without water, to assess their influence on augmenting heat transfer.

A committed team of researchers conducted a comprehensive examination of this challenge, employing both experimental and numerical approaches in their pursuit of an efficient remedy. Nonetheless, due to the inherent relationship between heightened pressure drop and improved heat transfer, attaining an ideal form is not always attainable. The scientific literature has extensively delved into a variety of twisted tape configurations, including alternate axis, cutting-bending-cutting off, clockwise and counter-clockwise arrangements, embossing, loose fit, multiple channels, multiple twisted tapes, perforation, regularly spaced, short length, changeable tape width, and varying twist ratio [10].

Oni and Paul [11] carried out a numerical study on twisted tape configurations with alternate-axis triangular cuts. They established empirical relationships based on their findings. Their research revealed that employing this particular design in a standard tube led to an enhancement in thermal efficiency of up to 1.43 times when compared to a conventional twisted tape.

In their study, Saysroy and Eiamsa-ard [12] conducted a numerical analysis of a multi-channel twisted tape configuration in both laminar and turbulent flow conditions, varying the number of channels from 2 to 8. The most favorable results were generally observed when employing two channels that corresponded to the twisted tapes. Another investigation focusing on multi-channel twisted tape found that a tape width smaller than the pipe diameter promoted laminar flow [13]. Additionally, Eiamsa-ard et al. [14] investigated the influence of twin-counter/co-twisted tapes on the heat transfer efficiency of a heat pipe, illustrating that the use of twisted tape in a heat exchanger can substantially decrease its overall dimensions.

Furthermore, twisted tape configurations offer a more straightforward layout compared to heated wire matrices, springs, fins, and similar structures. This simplicity makes them an attractive option for applications involving fouling [15-18]. Swirl flow devices [19], which encompass twisted tapes, are typically crafted from thin metallic strips and can be composed of various materials. The twisted tape insert stands out as a highly promising means of generating swirls, benefiting heat transfer in both smooth and turbulent flows. It instigates lateral mixing, resulting in a swirling motion or vortex within the heat exchanger, thereby enhancing the efficiency of heat transfer. This leads to an effective disruption of the thermal barrier layer and the breakdown of the viscous sublayer. Moreover, a twisted tape heat exchanger boasts the advantage of being easily and cost-effectively adaptable for integration into existing plain tube heat exchangers. The rotational movement caused by a coiled tape disrupts the flow patterns, leading to enhanced contact between the tube's surface and the passing fluid. This heightened temperature contrast brings about a greater efficiency in heat transfer, facilitated by better mixing of the fluid.

Dagdevir and Ozceyhan [20] carried out an experimental investigation to assess the heat transfer and thermal-hydraulic performance of a heat exchanger tube using various types of tapes. These included plain twisted tape, perforated twisted tape, and dimpled twisted tape. All the tapes shared the same dimensions, with a width and length of 17 mm and 100 mm, respectively. The holes and dimples in the two types of tapes had an 8 mm diameter. They also varied the pitch length for the perforated tape (PP) and the dimpled tape (Pd) to 25 mm, 50 mm, and 100 mm, and the pitch ratio of

the tapes (PP/H and Pd/H) was set at 0.5, 0.25, and 1. During the experiment, they used a mixture of water and ethylene glycol with different volume ratios (EG: W = 0:100, 20:80, and 40:60) as the working fluid. The Reynolds numbers ranged from 5217 to 22754, allowing comparison with a plain tube.

The results demonstrated that all types of twisted tapes outperformed the plain tube in terms of heat transfer coefficient, irrespective of the volume ratios of water and ethylene glycol. Specifically, the dimpled twisted tape with a pitch ratio of Pd/H = 0.25 achieved the highest Nusselt number at the highest Reynolds number and the highest efficiency at the lowest Reynolds number. This was especially notable with a value of 1.4 for the volume ratio of 0:100 water and ethylene glycol. These findings led to the conclusion that the addition of ethylene glycol did not significantly impact efficiency and heat transfer.

Tusara et al. [21] employed Computational Fluid Dynamics (CFD) software in their investigation, examining the impacts of varying twist ratios of a plain twisted tape within a tube. The twist ratios, denoted as y, were set at 3.46 and 7.6. The tube measured 900 mm in length with a diameter of 26.6 mm, while the tape had dimensions of 21 mm in width and 1 mm in thickness. The tube contained air at 300 K, and a constant heat flux of 8000 W/m² was applied to its wall. The Reynolds number spanned from 3642 to 21857. The objective of the research was to comprehend how different twist ratios influenced the friction factor, Nusselt number, and thermal performance factor.

In the case of y = 3.46, the friction factor surged by 185% to 245%, accompanying a 20% to 62% rise in the Nusselt number. This led to an escalation of the thermal performance factor from 0.9 to 1.2. As for y = 7.6, the friction factor saw an increase of 128% to 183%, with a 10% to 30% upturn in the Nusselt number. Consequently, the thermal performance factor advanced from 0.95 to 1.05. These findings suggest that lower twist ratios and Reynolds numbers result in more substantial enhancements in heat transfer and greater efficiency in the thermal performance factor.

Kim et al. [22] investigated heat transfer in turbulent flow using water as the medium, covering Reynolds numbers spanning from 10,000 to 20,000. They applied a consistent heat flux to the inner surface of the pipe and compared two scenarios: one with a twisted tape inside the flow tube and the other with a helical tube containing a twisted tape within the flow tube. The findings demonstrated that the helical tube incorporating the twisted tape displayed superior heat transfer efficiency. The most effective twist ratio was determined to be 7.86 for the helical tube with the twisted tape, surpassing other twist ratios. The study concluded that the Nusselt number was directly proportional to the Reynolds number and inversely proportional to the friction factor.

Balaga et al. [23] conducted a thorough investigation into the integration of various types of twisted tapes with wire coils within a circular flow tube. The study examined both plain and perforated tapes, each with different twist ratios denoted as y = (3, 4, 5), as well as twist ratios for the wire coil marked as CR = (3, 4). Water served as the working fluid under turbulent flow conditions, with Reynolds numbers ranging from 3000 to 16000. The study combined wire coils with plain twisted tapes of varying twist ratios, and also with perforated twisted tapes, placing these configurations inside a circular tube for comparison with a standard tube.

The results showed a substantial increase in heat transfer for the plain twisted tape with a twist ratio of y = 3 and CR = 3, with enhancements ranging from 65.06% to 101.13%. The friction factor also displayed improvements within the range of 2.75% to 30%. The presence of holes in the perforated twisted tape combined with wire coils led to even better heat transfer performance compared to the plain twisted tape, attributed to increased fluid turbulence within the circular tube. Heat transfer enhancement ranged from 75.67% to 177.81%, with friction factor improvements between 9% and 28% compared to the plain tube. The thermal performance factor was determined to be 2.03 for the plain twisted tape and 2.66 for the perforated twisted tape.

Wei et al. [24] undertook a study where they examined two variations of flat tapes positioned within a heat exchanger tube. The initial tape measured 19 mm in width, while the second tape was 8 mm wide. Both tapes were identical in length and

thickness. The heat exchanger tube itself measured 332 mm in length and had a diameter of 38 mm. A simulation was conducted employing a water-nano fluid blend, resulting in a Reynolds number range of 3000 to 6000, signifying turbulent flow. A constant heat flux was enforced on the tube wall. The wider tape was inserted into the heat exchanger tube, while in another tube, two 8 mm wide tapes were utilized. Remarkably, the Nusselt number showed an enhancement to 95 at a Reynolds number of 3000 when water was employed as the working fluid, in the absence of a twisted tape within the heat exchanger tube. However, with two tapes and the fluid mixture in the heat exchanger, the Nusselt number surged to 218 at a Reynolds number of 36000. This led to the conclusion that as the Reynolds number increased, so did the Nusselt number. Additionally, a tube containing two twisted tapes demonstrated a higher Nusselt number compared to a tube with just one twisted tape. The Performance Evaluation Criterion (PEC) efficiency was recorded at 2.18 for the tube equipped with a single twisted tape, whereas for the tube with two twisted tapes, the PEC efficiency was slightly lower at 2.04. This indicates that the use of a single twisted tape proved more effective for heat transfer than employing two twisted tapes.

Yongfeng et al. [25] investigated different configurations of partially twisted tapes situated within a three-dimensional circular tube of a heat exchanger. The main objective of this research was to attain optimal heat transfer efficiency while minimizing resistance, employing a Nano fluid mixture (Water/Al2O3) as the fluid medium within the tube. The Reynolds number ranged between 250 and 1000, signifying a regime of smooth, predictable flow. The tube wall received a constant heat flux of 5000 W/m². When liquid water was utilized as the primary flow medium within the tube, the Nusselt number experienced an increase from 15.13 to 28.42, whereas the friction factor rose from 0.022 to 0.052 at a Reynolds number of 1000, with semi-twisted tapes varying from 0 to 4. In the range of 0-3%, enhancements in the friction factor and the Nusselt number were 2.29% and 6.41% higher, respectively. At Re=750, utilizing four semi-twisted tapes at the same concentrations led to the highest Performance Evaluation Criterion (PEC) efficiency of 1.66.

Sagar et al. [26] conducted a study on heat transfer characteristics within a heat exchanger tube using two types of twisted tapes. One was a constant pitch twisted tape

made of aluminum and stainless steel, while the other was a variable pitch (4-3-4) tape of the same metal composition. The investigation encompassed both experimental and numerical analyses, employing water as the working medium in both cases. The twisted tapes measured 1.5 meters in length and 16 millimeters in width. The findings demonstrated that the variable pitch aluminum twisted tape outperformed the plain and constant pitch counterparts in terms of heat transfer quantity and coefficient. There was a notable enhancement in heat transfer (67.14%) for the constant pitch aluminum tape compared to the plain tube. Furthermore, the variable pitch aluminum tape exhibited an 18.15% increase in heat transfer compared to the constant pitch aluminum tape. A similar trend was observed for the variable pitch stainless steel tape, which demonstrated a 15.25% improvement in heat transfer and coefficient compared to the constant pitch stainless steel tape. The experimental results were in line with those obtained through Computational Fluid Dynamics (CFD) simulations.

Sami et al. [27] performed a numerical investigation on the heat transfer characteristics and friction factor in a heat exchanger tube employing two distinct types of twisted tapes exhibiting varying features. The tube's dimensions were 180 cm in length and 2.54 cm in diameter. The initial type of tape employed was the conventional twisted tape (CTT), and the second type was the parabolic-cut twisted tape (PCT). Both tapes possessed different twist ratios (y = 2.93, 3.91, and 4.89). The PCT tape featured three different depths (w = 0.5, 1, and 1.5 cm). The simulation incorporated a Nano fluid (CuO-water) with varying volumetric concentrations (2% and 4%). The outcomes demonstrated that under specific conditions, the CTT attained the highest Nusselt number (56) at the maximum Reynolds number (Re=2500), whereas the PCT tape achieved even higher values. The study concluded that the parabolic-cut twisted tape (PCT) surpassed the classical twisted tape (CTT) in terms of heat transfer performance.

Yadav and Padalkar [28] conducted a study utilizing Computational Fluid Dynamics (CFD) simulations to investigate heat transfer characteristics and performance within a heat exchanger tube. This investigation encompassed a turbulent Reynolds number range of 25,000 to 110,000, with heat flux applied to approximately two-thirds of the tube wall, ranging from 3200 to 6200 W/m^2. The study involved four types of tubes: three equipped with twisted tapes and one without. The first twisted tape was

positioned in the initial half of the heating zone (HLUTT), the second in the latter half of the heating zone (HLDTT), and the third tape spanned the entirety of the heating zone (FLTT). The findings revealed that the tube with the fully-length twisted tape (FLTT) demonstrated a notable enhancement in both heat and pressure transfer coefficients, increasing by 29% to 86% and 203% to 623%, respectively, in comparison to the plain tube lacking a tape. The HLUTT tube exhibited higher coefficients of heat and pressure transfer compared to the regular tape-free tube, with increments of 8% to 37% and 36% to 170%, respectively. Regarding the HLDTT tube, the heat and pressure transfer coefficients were elevated by 9% to 47% and 31% to 144%, surpassing those of the plain tube.

Vamsi and Chuen [29] conducted a study centered on the heat transfer characteristics within a heat exchanger tube. Specifically, they investigated the impact of different twisted tapes with varying shapes. The flow within the tube exhibited turbulence, with a Reynolds number ranging from 41,000 to 74,000. The researchers assessed how corrugated tube configurations influenced the efficiency, cost-effectiveness, and reduction of CO2 emissions in the recovery of exhaust heat from a heavy-duty diesel generator. In this context, the exhaust constituted one-third of the consumed fuel. The outer tubing was smooth, while the inner tubing featured both smooth and twisted segments along with an annular corrugation insert. Through simulations, they identified the most effective design, which incorporated a corrugated concentric heat exchanger with a twisted tape. They explored various iterations of twisted tapes, including perforated and twisted versions.

The study revealed that incorporating a twisted tape into a corrugated tube heat exchanger resulted in a 67% increase in heat transfer compared to a standard tube heat exchanger without a twisted tape. The use of twisted tape also led to a 35.3% boost in the heat transfer rate within the smooth tube. Notably, modified twisted tape (MTT) outperformed plain twisted tape (PTT) in the corrugated tube heat exchanger, achieving significantly higher heat transfer rates. When using twisted tape with rods (RTT), the performance of the annularly corrugated twist (ACT) improved by 126.17%. Combining ACT with RTT resulted in an annual fuel savings of 35.2%,

equivalent to 4,252 gallons of fuel per year, and reduced CO2 emissions by up to 43 metric tons.

This proposed system for recovering exhaust heat was found to be straightforward, relatively cost-effective, easy to install, and had no discernible impact on emissions specific to fuel. This makes it advantageous for the economy, particularly when implemented alongside the Ruby diesel power station. Extending this system to all diesel generators in rural areas, such as Alaskan villages, could lead to savings of up to 5.4 million dollars annually, based on a 370,000 MW-h power plant.

Haoxu et al. [30] conducted a comprehensive investigation, utilizing both numerical simulations and physical experiments, to examine the heat transfer properties and thermal-hydraulic effectiveness of a heat exchanger tube. This tube had specific dimensions, measuring 2400 mm in length and 16 mm in diameter. The study encompassed various types of twisted tapes, which were compared against a standard tube configuration. These tapes included a plain twisted tape, a tape with alternating clockwise and counterclockwise twists (referred to as ACCT), and a tape with evenly distributed semicircular cuts on both sides (referred to as ACCT for gap twist).

The degree of twisting, denoted as the twist ratio (y), was varied across all tape types (y = 3, 4, and 5). Water served as the working fluid in the experiments, with the Reynolds number ranging from 3500 to 9500.

The main findings of the study were as follows: In comparison to a plain untaped tube, all twist ratios of the twisted tapes resulted in higher heat transfer coefficients and friction coefficients. Specifically, a decrease in the twist ratio (y = 3) led to higher values for heat transfer coefficient, friction factor, and overall efficiency for all types of twisted tapes. Notably, the tape with alternating clockwise and counterclockwise twists (ACCT) demonstrated the highest heat transfer coefficient among all tested tapes. At the highest Reynolds number (Re = 9000), the ACCT tape achieved the highest Nusselt number (100), with a corresponding friction factor value of 0.27 at the

lowest Reynolds number (Re = 3600). Furthermore, the ACCT tape achieved the highest efficiency value, reaching 1.33.

In their study, Bipin and colleagues [31] conducted extensive research to investigate heat transfer, hydraulic thermal performance, and friction factor within a heat exchanger tube. They assessed the effectiveness of various twisted tape configurations, including plain twisted tapes with different twist ratios ranging from 2 to 6, and perforated twisted tapes with v-cut designs with twist ratios between 1 and 2. Copper was selected for both simulations and experiments, and air served as the working fluid. The Reynolds numbers spanned from 2700 to 23400. The results indicated that reducing twist ratios resulted in higher Nusselt numbers for all twisted tape variations, including solid and perforated types. Additionally, the friction factor decreased with higher twist ratios but exhibited an upward trend for solid and perforated tapes with v-cut designs. The Performance Evaluation Criterion (PEC) demonstrated improved performance with lower twist ratios across all types of tapes. These findings offer valuable insights for optimizing the efficiency of heat exchangers.

Sivasubramanian and their team [32] took into account cost, size, and simplicity when designing heat exchangers. They utilized various twisted tapes to examine their impact on enhancing heat transfer. For instance, they used an aluminum twisted tape with air as the flowing medium in a tube, adjusting parameters such as Reynolds number, twist ratios, thickness, width, and pitch ratio. This led to significant improvements in transfer efficiency and friction factor. A copper helical twisted tape exhibited similar results, with heat transfer efficiency increasing as the twist ratio decreased. When comparing different twist ratios, a ratio of 3 showed improved thermal efficiency and total solar intensity. The study also delved into stainless steel twisted tapes with varying parameters, showing increased Nusselt numbers, heat transfer, and friction factors as the twist ratio decreased. The research explored square ducting, highlighting higher performance ratios with full-length stainless steel twisted tapes compared to circular ducts, with square ducts exhibiting a 1.9 times higher friction factor.

Bhuiya et al. [33] carried out an investigation on a brass heat exchanger tube. They introduced two perforated twisted tapes with different levels of porosity (Rp = 1.2%,

4.6%, 10.4%, and 18.6%) and hole sizes (2 mm, 4 mm, 6 mm, and 8 mm). The study employed air as the fluid, exhibiting turbulent flow within Reynolds numbers spanning from 7200 to 50000. The findings revealed that as porosity decreased, there was an overall increase in heat transfer coefficient, friction coefficient, and thermal hydraulic efficiency, except at 1.2% porosity, where the improvement was marginal. The heat transfer rate saw a rise between 80% to 290%, while the friction factor increased by 111% to 335%. The highest efficiency of 1.44 was attained at 4.6% porosity, coinciding with the peak Nusselt number of 240 and friction factor of 0.135.

In a separate study, Reza and Ashkan [34] explored heat transfer, flow, and thermal hydraulic performance using water as the base fluid, combined with Nano fluids of AL2O3, CuO, and TiO2 at varying volumetric concentrations (1-4%). A tube with dimensions of 420 mm in length and 20 mm in diameter was employed, along with a tape featuring a width of 20 mm and a thickness of 2 mm. The heat application was set at 50,000 w/m2, and the simulation encompassed turbulent flow with Reynolds numbers ranging from 4000 to 12000. The combination of 4% volume ratio of Nano fluids with water resulted in the highest heat transfer values, yielding a thermal hydraulic efficiency of 1.54 and a friction factor of 0.225. CuO emerged as the most effective Nano fluid, offering the highest efficiency of 1.56.

Jian et al. [35] directed their attention towards the heat transfer performance and thermal performance factor of a heat exchanger tube. They employed numerical analysis involving three types of twisted tapes: a plain twisted tape with a width matching the inner tube diameter, a short-width twisted tape, and a center-cleared twisted tape. The study was carried out under laminar flow conditions, with Reynolds numbers ranging from 500 to 1750. The Nusselt number and thermal performance factor exhibited an upswing with higher Reynolds numbers, while the friction factor showed a decrease. The center-cleared twisted tape displayed superior heat transfer and thermal performance in comparison to the short-width twisted tape.

In a study conducted by Shiva et al. [36], the heat transfer characteristics and thermal hydraulic performance of a heat exchanger tube were examined using differently arranged twisted tapes. The first tube featured a single twisted tape, the second had

two twisted tapes swirling in the same direction, and the last one contained two tapes twisted in opposite directions. Various twist ratios (0.48, 0.52, 0.56) were applied to the two tapes with water flow conditions at Reynolds numbers ranging from 1000 to 2500. The results showed that at a twist ratio of 0.56, the counter-swirl twisted tape achieved the highest Nusselt number, surpassing both co-swirl configurations. The counter-swirl configuration also had a slightly higher friction factor. Moreover, the thermal hydraulic performance efficiency was superior for all double twisted tape configurations compared to a single twisted tape. Specifically, the counter-swirl configuration at a twist ratio of 0.56 exhibited the highest efficiency, with a value of 1.95.

Hamed and Farzad [37] conducted a comparative analysis between circular and flat tubes using water and AL2O3 Nano fluid to determine the most effective option in terms of heat transfer and thermal hydraulic performance. The study covered a range of Reynolds numbers from 100 to 2000. The flat tube with a single twisted tape (plain) using the nanofluid exhibited the highest efficiency and also recorded the highest friction factor at the lowest Reynolds number for the same tape. The highest Nusselt number was observed at the highest Reynolds number. Three types of flat tubes were investigated: one with a single twisted tape, another with two twisted tapes in the same direction (Dual Co-twisted tape), and the last one containing two double counter-twisted tapes. For the Dual counter-twisted tape, the highest hydraulic thermal efficiency (1.15) was achieved at the lowest Reynolds number, along with the highest friction factor (0.69). The highest Nusselt number for this tape was obtained at the largest Reynolds number. The Dual co-twisted tape achieved the second-best efficiency (1.13) at the lowest Reynolds number, while the single twisted tape exhibited the lowest efficiency (1.07) at the lowest Reynolds number as well.

Zheng et al. [38] explored the effectiveness of a heat exchanger tube modified with a dimpled and twisted tape, studying its heat transfer and thermal hydraulic performance. The tube in question measured 840 mm in length and 20 mm in diameter, while the twisted tape had dimensions of 20 mm in width and 1 mm in thickness. They employed an AL2O3-water Nano fluid for their investigation, analyzing both the dimpled and protrusion sides while considering Nano fluid volume fraction (a) and

nanoparticle diameter (Dp). The results indicated significant enhancements in heat transfer on both the dimple and protrusion sides, with the dimple side showing superior performance. The use of dimples increased convective heat transfer by 25.53% compared to a smooth tape, promoting turbulence and heat transfer. Introducing Nano fluids further improved heat transfer, with a maximum increase in heat transfer coefficient (h) of 58.96%. A smaller nanoparticle diameter (Dp) led to even better heat transfer performance, albeit with a slight increase in resistance. However, the effect of (Dp) became negligible after exceeding 40 nm.

Chinaruk et al. [39] conducted an extensive study on heat exchanger tubes, comparing three tube configurations regarding their heat transfer characteristics and friction factor. The first tube featured a dimpled surface with varying pitch ratios (0.7 and 1) and included twisted tapes with different twist ratios (3, 5, 7). The second tube had a dimpled surface but lacked twisted tape, while the last tube was a conventional smooth-surfaced tube. The study used air as the working fluid, covering a range of Reynolds numbers from 12,000 to 44,000. The results demonstrated that the dimpled tube with twisted tape, especially at the lowest twist ratio (3) and a pitch ratio of 0.7, outperformed both the dimpled-only tube and the smooth tube in terms of heat transfer. The highest Nusselt number (440) was achieved under these conditions, with the highest friction factor recorded at approximately 0.26.

Nakhchia and Esfahanib [40] delved into the heat transfer properties and hydraulic thermal performance of heat exchanger tubes utilizing twisted tape with specific rectangular cuts. They explored single and double rectangular cuts with varying cut length ratios (b / w) from 0.25 to 0.75 and cut-width ratios (c / w) ranging from 0.25 to 1. Water served as the working fluid, with Reynolds numbers spanning from 5000 to 16000. The tube used in the simulation had a length of 840 mm and a diameter of 26.2 mm. The findings revealed that the highest Nusselt number was attained with a single-cut twisted tape at a cut length ratio (b / w = 0.75) and cut width ratio (c / w = 0.5), reaching a value of 240 at the highest Reynolds number. In the case of double-cut twisted tape, the highest Nusselt number was observed at a cut length ratio (b / w = 0.25) and cut width ratio (c / w = 1), with a value of 230. These conditions also corresponded to the highest friction factors. The highest efficiency was achieved with

a single-cut twisted tape at a cut length ratio (b / w = 0.75) and a specific cut width ratio (c / w), with a value of 1.64.

Ahmed's study [41] examined the heat transfer and thermal hydraulic performance of a heat exchanger tube. This study involved the use of twisted tapes with square and rectangular cross-section dimensions, specifically measuring (1 mm * 1 mm), (1 mm * 2 mm), (1 mm * 2.5 mm), and (1 mm * 3 mm). The research compared the tube's performance with and without these tapes inserted. The tube used for simulation had a length of (1920 mm) and a diameter of (11.08 mm), with water as the working fluid. The Reynolds number varied from 1500 to 24000, and a heat flux of (800 w/m2) was applied to the tube wall. The findings indicated that the twisted tape measuring (1 mm * 3 mm) achieved the highest heat transfer percentage, along with the highest Nusselt number, reaching a value of 21. Additionally, the (1 mm * 3 mm) twisted tape had the highest friction factor, registering at 0.7.

Suvanjan and Himadri [42] investigated the thermal hydraulic performance of a heat exchanger tube employing a plain twisted tape with different twist ratios (y = H / D) and diagonal diameter ratios (d = w / D). These values were (15, 45) for the twist ratio and (0.83, 0.75, 0.66) for the diagonal diameter ratio. The Reynolds number in the simulation ranged from 100 to 20000. The study revealed that the highest thermal hydraulic efficiency occurred at a twist ratio of (y = 15) and a diameter ratio of (d = 0.75), with an efficiency value of 1.19. Furthermore, the same twist ratio (y = 15) combined with a diameter ratio of (d = 0.66) also yielded the highest efficiency of 1.19.

Yuxiang et al. [43] conducted research on the heat transfer characteristics and thermal hydraulic performance of a spiral groove tube (SGT) heat exchanger. They utilized plain twisted tapes with small and large widths (10 mm and 15 mm), positioning two opposite tapes inside the spiral tube in a twin overlapped twisted tape configuration. This involved different twist ratios (P1/P2) ranging from (1.06 to 3.22). The pitch of the small tape was fixed at (36 mm), while the pitch of the large tape varied (38 mm, 56 mm, 88 mm, and 116 mm), resulting in variable twist ratios (y = 2.53, 3.73, 5.87, and 7.73). Stainless steel was used as the tape material, and air was the working fluid,

with a Reynolds number range of (8000 - 22000). The study compared the presence of these tapes inside the spiral groove tube with a smooth spiral groove tube without tapes. The results demonstrated that reducing the twist ratio of the two tapes inside the spiral groove tube (P1/P2 = 1.06) enhanced heat transfer, with the Nusselt number reaching a value of 117. The highest friction factor was also observed at the same ratio, amounting to 0.63. Interestingly, the spiral groove tube without a twisted tape achieved the highest hydraulic thermal efficiency, with a value of 1.14. For the four tapes, the efficiency ranged between 0.87 and 1.08.

Dagdevir et al. [44] examined the heat transfer characteristics and thermal hydraulic behavior of a heat exchanger tube using various types of modified tapes. These included standard twisted tapes, perforated twisted tapes placed at the tube's edge (p), and twisted tapes with indentations at the edge (p). They explored different values of (p = 25, 50, and 100) mm, while maintaining a fixed pitch distance (H = 100 mm), tape width (17 mm), thickness (1 mm), and twist ratio (y = 5.88) for all tapes. Three (p/H) ratios were employed, specifically 0.25, 0.5, and 1. A comparison was drawn between tubes equipped with these tapes and a smooth untaped tube. The tube used in the study was 1 meter long, with an inner diameter of 17 mm and an outer diameter of 21 mm. Water served as the working fluid, and the Reynolds number spanned from 6000 to 33000. A consistent heat flux was applied to the tube wall. The findings revealed that the dimpled twisted tape with a (p/H) ratio of 0.5 led to the highest heat transfer, yielding a Nusselt number of 300 and a friction factor of 0.96. Moreover, this same tape achieved the highest hydraulic thermal efficiency with a value of 1.58.

Thianponga et al. [45] conducted a study on the heat transfer properties and thermal hydraulic performance of a heat exchanger tube utilizing perforated twisted tape with parallel wings. The pitch length of the tape remained constant at 56 mm, with a tape width of 18 mm and a twist ratio (y) set at 3. They employed three different hole diameters on the tape, resulting in hole diameter ratios (d/W) of 0.11, 0.33, and 0.55. The wing depth ratio (w/W) ranged from 0.11 to 0.33. The Reynolds number varied from 5500 to 20500. The results indicated that the most effective heat transfer occurred when the hole diameter was smaller (d/W = 0.11) and the wing depth was larger (w/W = 0.33). The highest Nusselt number, approximately 275, was achieved at these

specified ratios. Furthermore, the highest thermal efficiency PEC was attained under these conditions, with a value of 1.32.

Nakhchia et al. [46] studied the heat transfer characteristics and thermal-hydraulic performance of a heat exchanger tube by incorporating a double-cut twisted tape (DCTT) inside. The tube had dimensions of 840 mm in length, 22.6 mm inner diameter, and 26.6 mm outer diameter. The twisted tape had a width (W) of 20 mm, a fixed pitch length (H) of 105, and a twist ratio (y) of 5.25. Cuts of varying depths (b = 2.5, 5, 7.5, and 9 mm) were made on the tape, with a consistent cut width (c = 10 mm), on both sides relative to the twisted tape. The cutting ratio (b/c) ranged from 0.25 to 0.9. Water was used as the working fluid, with Reynolds numbers spanning 5000 to 15000. Results revealed that all cut ratios of the twisted tape exhibited higher Nusselt numbers compared to the plain tube. The greatest Nusselt number, around 275, was attained at the highest cut ratio (b/c = 0.9) and the largest Reynolds number. The highest friction factor was observed at the lowest Reynolds number for the same ratio, registering at 0.31. The utmost thermal-hydraulic efficiency, at 1.63, was achieved at the highest cutting ratio (b/c = 0.9), while the second-best efficiency was noted at a ratio of 1.52 (b/c = 0.75).

Mushatet et al. [47] performed an extensive investigation on the heat transfer properties and thermo-hydraulic behavior of a heat exchanger tube utilizing an enlarged tapered twisted tape (ITTT) within the tube. The tube measured 1000 mm in length and 20 mm in diameter. The width of the tapered twisted tape ranged from 1 mm to 18 mm, starting at 1 mm and ending at 18 mm. The tape's length remained fixed at 90 mm, and the twist ratio (y) was 5. The length of the tapered twisted tape varied from 250 mm to 1000 mm. Air was employed as the working fluid, with Reynolds numbers ranging from 10000 to 40000. Findings demonstrated significant enhancements in heat transfer, with the Nusselt number increasing by 75% through experimental means and 100% through numerical simulations for the tapered twisted tape measuring 250 mm in length and with widths ranging from 1-18 mm at a Reynolds number of 10000. The friction factor saw a 220% experimental increase and a 226% numerical increase for the same tape. The hydraulic thermal efficiency also

experienced substantial improvements, with a 1.19-fold experimental increase and a 1.37-fold numerical increase for the mentioned tape.

Bucak and Yılmaz [48] conducted a numerical investigation into the heat transfer characteristics and thermo-hydraulic performance of a heat exchanger tube. They employed a twisted tape featuring a periodic arrangement of spherical dimples and protrusions. The study encompassed various configurations involving dimples, protrusions, and a combination of both, employing different tape designs. The Reynolds numbers spanned from 3000 to 27000. The patterned twisted tapes exhibited superior heat transfer and Nusselt numbers compared to the plain tube. Specifically, the patterned twisted tape with densely packed dimples and protrusions (D-DPT) achieved the highest Nusselt number, reaching 370 at the highest Reynolds number. Furthermore, the patterned twisted tape with dense protrusions (D-PT) registered the highest friction factor at the lowest Reynolds number, measuring 0.52. As for hydraulic thermal efficiency, the patterned twisted tape with dense dimples and protrusions (D-DPT) secured the highest value of 1.51, while the second-highest efficiency, at 1.48, was observed in the patterned twisted tape with dense protrusions (D-PT).

Muhammad et al. [49] conducted both numerical and experimental investigations into the heat transfer properties and thermal hydraulic performance of a heat exchanger tube. They utilized perforated triple twisted tapes with varying porosities (Rp = 1.2%, 4.6%, 10.4%, and 18.6%). The holes in the tapes ranged in diameter from 2 mm to 8 mm, with hole spacings of 16.25 mm and 25 mm. The twisted tape had a width of 32.5 mm, and the twist ratio was (y / w = 1.92). The working fluid used was air, and a constant heat flux was applied to the tube's wall. The Reynolds number varied between 7250 and 49800. Results indicated that all the triple perforated twisted tapes exhibited higher heat transfer and Nusselt numbers compared to the plain tube. The highest Nusselt number (240) was achieved at the highest Reynolds number for the twisted tape with a porosity of 4.6% (Rp = 4.6%). Additionally, the maximum pressure value (300 N/m2) was recorded at the highest Reynolds number for the same porosity. The highest friction factor (0.145) was observed at the lowest Reynolds number for the same porosity. The highest thermal hydraulic efficiency was attained at the lowest

Reynolds number (1.5), with the second-highest efficiency (1.48) recorded at a porosity of 1.2% (Rp = 1.2%).

Nanan et al. [50] conducted an experimental investigation on a heat exchanger tube's heat transfer characteristics and thermal hydraulic performance. They employed helical twisted tapes made of aluminum, which were perforated and had varying diameter ratios (d / w = 0.2, 0.4, and 0.6), along with different ratios of perforation pitch (s / w = 1, 1.5, and 2), helix pitch ratio (P / D = 2), and twist ratio (y = 3). A comparison was made between these perforated helical twisted tapes and a plain tube. The Reynolds number spanned from 6000 to 20000. The results demonstrated that all perforated helical twisted tapes exhibited superior heat transfer performance compared to the plain tube. The highest Nusselt number (around 83) was achieved at the highest Reynolds number, specifically for the helical pitch ratio (P / D = 2) and the twist ratio (y = 3). The maximum friction factor (0.175) was recorded at the lowest Reynolds number for the same ratios. The highest hydraulic thermal efficiency (1.29) was attained at the ratio (P / D = 2) and the twist ratio (y = 3), while the second-best thermal efficiency (1.27) was observed at a diameter ratio of 0.2 (d / w = 0.2) and a perforation pitch ratio of 1.5 (s / w = 1.5).

Bhuiya et al. [51] conducted a similar experimental study on a heat exchanger tube's heat transfer properties and thermal performance coefficient. They utilized twisted perforated tapes with different perforation diameters (3 mm, 5 mm, 7 mm, and 9 mm), resulting in varying porosities (RP = 1.6%, 4.5%, 8.9%, and 14.7%). The holes were positioned at distances of 20 mm axially and 16.25 mm transversely. The tube, constructed of brass, had dimensions of 1500 mm in length, 70 mm inner diameter, and 90 mm outer diameter. The twisted tape, composed of stainless steel, measured 1500 mm in length, 65 mm in width, and had a twist ratio of 1.92. A comparison was drawn between the tube with this tape and a plain tube devoid of the tape. Air served as the working fluid, and the Reynolds number ranged from 7200 to 49800. A consistent heat flux was applied to the tube's wall. The results revealed that all twisted tapes with varying porosities exhibited superior heat transfer compared to the plain tube. The highest Nusselt number (288) was attained at a porosity of 4.5% (Rp = 4.5%) at the highest Reynolds number. At this same porosity, the highest friction factor

(0.145) was recorded at the lowest Reynolds number. The highest thermal performance factor was achieved under the same porosity and the lowest Reynolds number, with a value of 1.58.

Hasanpour et al. [52] conducted an experimental investigation on a heat exchanger tube with a corrugated design measuring 1500 mm in length, 16 mm in inner diameter, and 56 mm in outer diameter. They employed twisted tapes made of aluminum, possessing twist ratios of 3, 5, and 7, and hole diameters with ratios of 0.11 and 0.33. These tapes featured either V-cut or U-cut shapes, with width-to-depth ratios ranging from 0.3 to 0.6. Water served as the working fluid, and Reynolds numbers spanned from 5000 to 15000. The results demonstrated that the Nusselt number for all corrugated tubes with twisted tapes (TT) was significantly higher compared to plain corrugated tubes across the entire range of Reynolds numbers studied. Both V-cut and U-cut TTs exhibited superior Nusselt numbers compared to normal TTs. The most substantial enhancement was observed at a twist ratio of 3 for V-cut tape with a width ratio (wr) of 0.3 and depth ratio (dr) of 0.45. Regarding pressure drop, the use of V-cut TT in a corrugated tube led to a greater friction factor value compared to standard TT or an empty corrugated tube. Similar trends were noted with U-cut twisted tape, which produced a higher friction factor value than plain twisted tape or an empty tube. Alterations in width ratio and depth ratio had an impact on the friction factors for both V-cut and U-cut tapes.

Nakhchi and Esfahani [53] conducted a computational analysis on a heat exchanger tube employing a double V-cut twisted tape within. The tube measured 840 mm in length and 25 mm in diameter. The twisted tape had a width of 20 mm, a pitch length of 105 mm, and a fixed cutting width of 5 mm, with varying cut depths (3 mm, 5 mm, 7 mm, and 9 mm). The cutting ratio (b / c) ranged from 0.6 to 1.8. They utilized a CuO-water Nano fluid with different volumetric concentrations (ranging from 0% to 1.5%). Reynolds numbers were within the range of 5000 to 15000. The findings indicated that all double V-cut configurations yielded higher heat transfer enhancement compared to plain twisted tape without cuts. The highest Nusselt number (approximately 320) was attained at the cut ratio (b / c = 1.8) and a Nano-volume concentration of 1%. Moreover, at the same cut ratio and volumetric concentration, the highest friction

factor (0.25) was obtained at the lowest Reynolds number. The highest thermal hydraulic efficiency (2) was achieved at a Nano-volume concentration of 1% and the lowest Reynolds number.

Khalil et al. [54] conducted a comprehensive study, combining numerical simulations and practical experiments, aimed at enhancing the heat transfer and thermal hydraulic efficiency of a heat exchanger tube. This was achieved by introducing four twisted tapes. The tube utilized in the experiment had specific dimensions: a length of 1000 mm and a diameter of 20 mm. Four distinct twist ratios (y = 2.5, 3, 3.5, and 4) were tested, covering a Reynolds number range from 1000 to 18000. The findings indicated that all twist ratios led to improved heat transfer in comparison to a plain untampered tube. Notably, the tube containing a single twisted tape exhibited the highest Nusselt number (240) and pressure (3000 N/m2) at the highest Reynolds number (18000) for a twist ratio of 2.5. Additionally, the tube equipped with a double twisted tape in a co-swirl configuration achieved a Nusselt number of 265 and pressure of 4000 N/m2 under the same conditions. The tube with a double twisted tape in a counter-swirl arrangement demonstrated the highest Nusselt number (290) and pressure (4250 N/m2) at a twist ratio of 2.5 and the highest Reynolds number (18000). The most effective configuration, with an effectiveness value of 0.42, was attained using the double twisted tape in a counter-swirl arrangement at a twist ratio of 2.5.

Dhumal et al. [55] concentrated their research on an experimental investigation of the heat transfer characteristics of a heat exchanger tube employing twisted tapes with varying twist ratios (y = 4.21, 5.33, and 6.46), with water as the working fluid. The study incorporated theoretical analysis to assess the convective heat transfer performance and fluid flow attributes within a double-pipe heat exchanger. The outcomes revealed an inverse relationship between the twist ratio and the Nusselt number, while concurrently observing a decrease in pressure drop. Although the incorporation of inserts in a heat exchanger resulted in augmented heat transfer rates, it was noted to induce an elevation in the exchanger's pressure drop. This elevated pressure drop necessitates higher pumping power, consequently contributing to elevated overall operational expenses.

Feizabadia et al. [56] carried out an experimental inquiry into the heat transfer characteristics and thermal performance index of a heat exchanger tube using two distinct tube configurations: a smooth tube and a U-shaped tube. In both cases, twisted tape was inserted, featuring twist ratios of 2 and 6. The tube dimensions for the experiment were as follows: length of 1000 mm, inner diameter of 15.2 mm, and outer diameter of 17.2 mm. The U-shaped tube maintained a fixed twist ratio of 0.65. The twisted tape possessed a small pitch length of 30 mm, a large pitch length of 90 mm, and a width of 15 mm. Water was employed as the working fluid, and the Reynolds number spanned from 3843 to 11436. The findings illustrated that all twist ratios resulted in a higher heat transfer coefficient compared to the smooth tube without tape. The peak Nusselt number (170) was achieved at the lowest twist ratio (y = 2) for the twisted U tube at the highest Reynolds number. The highest friction factor (0.077) was observed at the same lowest twist ratio (y = 2) for the twisted U tube but at the lowest Reynolds number. The greatest efficiency value (1.9) was obtained under similar conditions, emphasizing the significance of the low twist ratio (y = 2) for the twisted U tube at the lowest Reynolds number.

Suvanjan et al. [57] conducted an experimental investigation into the heat transfer properties and thermal performance of a corrugated tube equipped with a spring tape. They explored two different corrugation pitch ratios, denoted as y = P / D (0.7 and 1), and three spring ratios, defined as s = H / W (3, 5, and 7). The experimental fluid was air, and the Reynolds number ranged from 10,000 to 50,000. The study compared the corrugated tube with a spring tape, the corrugated tube without a spring tape, and the plain tube. The findings revealed that all pitch ratios, when combined with the spring tape, exhibited higher heat transfer values compared to the plain tube. The ratio (y = 0.7) and spring ratio (s = 3) produced the highest Nusselt number at the highest Reynolds number, reaching 300. The maximum friction factor was attained at the same ratio (y = 0.7) and spring ratio (s = 3), but at the lowest Reynolds number, registering at 0.075. The highest efficiency value was also achieved at the ratio (y = 0.7) and spring ratio (s = 3), with a value of 2.8. The second-highest efficiency was observed at (y = 0.7) and (s = 5), measuring 2.25.

Naga et al. [58] conducted an experimental analysis of the heat transfer properties and thermal hydraulic performance of a heat exchanger tube employing twisted tapes with varying twist ratios (3, 4, and 5). Each twist ratio involved tapes with different widths ranging from 10 mm to 26 mm. These tapes were compared within the heat exchanger tube against a plain tube without tapes. Air served as the working fluid, and the Reynolds number varied between 6,000 and 13,500. The results demonstrated that all straight tapes with different widths exhibited higher heat transfer values compared to the plain tube. The highest Nusselt number (33) was achieved at the highest Reynolds number for the straight tape with the widest width (26 mm). The highest friction factor (0.0095) was also obtained at the lowest Reynolds number for the straight tape with the widest width (26 mm). Among the twist ratios, the tape with a twist ratio of (3) and a width of (26 mm) displayed the highest Nusselt number (47) at the highest Reynolds number. For the twist ratio (4) and width (26 mm), the highest Nusselt number was 40 at the highest Reynolds number. Finally, at the twist ratio (5) and width (26 mm), the highest Nusselt number was 38 at the highest Reynolds number. The highest efficiency (1.64) was recorded for the twist ratio (3) and width (26 mm).

In the study conducted by Yunmin et al. [59], an examination was carried out to assess the heat transfer characteristics and thermo-hydraulic effectiveness of a heat exchanger tube. They utilized a wavy-tape insert with a tapered center within a plain tube, comparing it to a plain wavy-tape. The simulated fluid used was water, with Reynolds numbers ranging from 600 to 1800. The tube's dimensions were a length of 500 mm and a diameter of 20 mm. The goal of the research was to identify the optimal operating conditions for the center-tapered wavy-tape insert. It was found that a greater waveform factor led to more efficient heat transmission. The amplitude ratios were constrained to a range of 0.3 to 0.7 for practical purposes, and the suitable period ratio fell between 2 and 2.5. These conditions resulted in notable enhancements, boosting the Nusselt number (Nu) by 5.23-8.99 times and the performance evaluation criterion (PEC) by 2.62 times. Empirical formulas were developed for Nu and the friction factor (f) based on the waveform factor, period ratio, and Reynolds number. The research outcomes were confirmed through Stereo-PIV (Particle Image Velocimetry) experiments. The center-tapered wavy-tape insert demonstrated superior overall thermo-hydraulic performance, especially when aiming for heightened heat transfer

and reduced flow resistance. This insert emerged as a viable approach for augmenting laminar convective heat transmission.

In the study by Akeel et al. [60], an experimental inquiry was conducted to explore the heat transfer attributes and thermal hydraulic performance of a heat exchanger tube employing a combination of fixed and rotating twisted-tapes. This combination comprised a stationary twisted-tape alongside a rotating one, which was powered by a motor at different speeds (200 RPM and 400 RPM). The tube's specifications were a length of 1200 mm, an inner diameter of 54 mm, and an outer diameter of 60 mm. The twisted tape measured 1200 mm in length and 25 mm in width, featuring varying twist ratios (y = 6 and 7.2). A comparison was drawn between the tubes fitted with these twisted-tapes and a plain tube lacking any tape. The experimental fluid used was air, with Reynolds numbers ranging from 8000 to 13000. The results demonstrated that all twist ratios and speeds of the twisted tapes yielded a higher heat transfer coefficient compared to the plain tube. The peak Nusselt number was attained at a high speed (400 RPM) and a low twist ratio (y = 6) at the highest Reynolds number (13000). Additionally, the highest friction factor value (0.035) was observed at high speed (400 RPM) and the lowest twist ratio (y = 6) for the lowest Reynolds number (8000). The highest efficiency was achieved at high speed (400 RPM) and low twist ratio (y = 6), registering at 1.45. The second-best efficiency was attained at low speed (200 RPM) and low twist ratio (y = 6), with a value of 1.43.

Humam [61] conducted a study involving both numerical and practical investigations to examine the heat transfer characteristics and thermal efficiency of a heat exchanger tube using two distinct tube designs. The initial tube was a smooth tube with a coiled tape featuring different twist ratios (y = 4 and 8). The second tube was a slotted dimple tube with an inserted coiled tape, also possessing different twist ratios (y = 4 and 8). Both tubes shared the same dimensions, measuring 1600 mm in length and 35 mm in diameter. The slotted dimple tube had additional specifications, including slots spaced 40 mm apart, with a diameter of 10 mm and a depth of 5 mm. A comparison was drawn between these two tubes and a plain tube lacking a coiled tape. The medium utilized was air, and the Reynolds number spanned from 4000 to 15000. The findings indicated that both tubes with twist ratios (y = 4 and 8) displayed elevated heat transfer

coefficients compared to the plain tube devoid of a coiled tape. The slotted dimpled tube with twist ratios (y = 4 and 8) achieved the highest Nusselt number, registering at 80 at the maximum Reynolds number (15000). The smooth tube with a twist ratio of 4 exhibited the highest friction factor value, reaching 0.45 at the highest Reynolds number. Furthermore, the slotted dimpled tube with twist ratios (y = 4 and 8) also demonstrated superior efficiency values, reaching 1.4 in contrast to the plain tube at the same twist ratio.

Yan et al. [62] conducted an experimental investigation to scrutinize the heat transfer properties and thermal-hydraulic performance of a heat exchanger tube employing a cross-hollow coiled tape inserted within the tube. The experiment encompassed turbulent flow conditions with Reynolds numbers varying from 5600 to 18000. The coiled tape was composed of nylon metal and came in different widths (6 mm, 8 mm, and 10 mm). The experimental medium was air. The results revealed that all the coiled tapes with varying widths provided higher heat transfer coefficients compared to a standard tube lacking any tape insert.

2.1. SUMMARY OF LITERATURE REVIEW

This chapter focuses on research aimed at enhancing the efficiency of heat transfer and thermal performance in heat exchanger tubes. The main goal was to boost the heat transfer coefficient, resulting in higher Nusselt numbers, while also maximizing overall thermal efficiency. By incorporating various types and configurations of twisted tapes within the heat exchanger tubes, each with distinct twist ratios, a thorough comparison was possible with plain, smooth tubes lacking tape.

Consistently, the key findings demonstrated that the inclusion of twisted tapes inside the heat exchanger tubes led to an augmentation of the heat transfer coefficient and an overall enhancement in thermal performance compared to plain tubes without tape. The twisted tapes induced disturbances in the fluid flow, creating vortices that generated a circular motion along the tape. This phenomenon facilitated improved contact between the tube's surface and the fluid, resulting in enhanced heat transfer.

Furthermore, it's worth noting that most of the researches conducted their experiments under turbulent flow conditions. This choice is significant, as turbulent flow often occurs in practical heat exchanger applications, making these findings highly relevant to real-world scenarios. The choice of fluid used in these experiments was primarily water or air, which are common fluids in heat exchanger applications.

In summary, the use of twisted tapes inside heat exchanger tubes has been demonstrated as an effective approach to enhance heat transfer efficiency and thermal performance, particularly in cases of turbulent flow. This research provides valuable insights for optimizing heat exchanger designs to achieve higher heat transfer rates while maintaining operational efficiency.

2.2.THESIS SUMMARY

This thesis constitutes a numerical investigation of an experimental study, as documented in reference [20]. This study employs three distinct types of twisted tapes, namely, plain twisted tapes, perforated twisted tapes, and dimple twisted tapes. Within the context of this thesis, the twist pitch length remains constant for all tapes, with the distinguishing factor being the length of the hole's pitch and the dimples pitch (25, 50, and 100 mm) for both the perforated tape and the dimple tape. The chosen approach within this thesis involves the utilization of turbulent flow, with water as the working fluid. The heat transfer enhancement using different types of the twisted tape inserts contributes to a deeper understanding of the effects of these twisted tape designs on heat exchanger performance, with potential implications for improving heat exchanger efficiency in real-world applications.

PART 3

MATERIAL AND METHOD

The present study constitutes a numerical investigation involving the use of three distinct types of twisted tape inserts, specifically: plain twisted tapes, perforated twisted tapes, and dimple twisted tapes inside a tube. The primary objective of this investigation is to assess the impact of these various twisted tape designs on heat transfer enhancement within a tube. The primary differentiating factor among these tapes was the varying length of the hole's pitch and dimples pitch, set at 25, 50, and 100 mm for both the perforated and dimple tapes. This deliberate design variation aimed to provide insight into the heat transfer performance characteristics associated with different tape configurations. In this part, several mathematical equations for heat exchanger solutions, such as the continuity equation, the momentum equation, the energy equation, the dissipation energy equation, and the kinetic energy equation will be dealt.

3.1. NUMERICAL PROCEDURE

Numerical simulations play a pivotal role in the development of applications related to fluid flow and heat transfer, encompassing a growing range of diverse fields. For many companies, computational fluid dynamics (CFD) has evolved into an indispensable consideration within the design process. The analysis of heat exchangers involves solving a series of coupled conservation equations for mass, energy, and momentum [63]. CFD enables the computation of critical parameters such as temperature, pressure, air velocity, water vapor content, as well as the determination of heat exchanger efficiency and heat transfer rates. Computers are employed to model the intricate interaction of liquids and gases with surfaces defined by boundary conditions. The utilization of high-speed supercomputers facilitates the discovery of more optimal solutions. Compared to traditional experimental investigations, CFD has

the advantages of simultaneously handling numerous system configurations, providing cost-efficient outcomes.

3.1.1. Governing Equations

The fundamental equations of fluid dynamics are rooted in the principles of conservation, particularly with the assumption of a Newtonian working fluid, such as water. The Navier-Stokes equations are crucial in characterizing the flow of this fluid, being guided by these universal laws of conservation. In the current study, both the Navier-Stokes and energy transfer equations govern the investigation of heat transfer and fluid flow.

Given that the working fluid is considered incompressible, factors such as thermal radiation, chemical reactions, and compression work are assumed to be negligible. The equations established by Stokes and Navier provide a comprehensive description of fluid behavior, including the equations for continuity, momentum, and energy, which are as follows:

- Conservation of Mass: This equation is derived from the application of the Conservation of Mass law to the fluid flow.
- Conservation of Momentum: The preservation of momentum law relies on Newton's Second Law of Motion. Applying this law to fluid flow yields a vector equation known as the momentum equation, which characterizes the flow behavior.
- Conservation of Energy: This legislation parallels the First Law of Thermodynamics, and the resulting fluid dynamic equation is known as the energy equation.

To fully define the system of equations, it is imperative to establish correlations between various fluid properties in addition to deriving equations from these universal principles. This comprehensive approach ensures a thorough understanding of the complex interactions within the fluid, facilitating accurate modeling and analysis.

3.1.1.1. Conservation of Mass

In a closed system, where matter and energy exchanges are absent, the fundamental law of conservation of mass dictates that the system's mass remains constant over time. This principle ensures that neither mass quantity can be added nor subtracted from the system, maintaining a consistent total mass within the system.

The rule of conservation of mass further specifies that while mass cannot be generated or destroyed, it can undergo spatial reorganization, leading to changes in the entities associated with it, albeit without altering the overall mass quantity.

The equation denoted as follows, expressed in a Cartesian coordinate system with u, v, and w representing the x, y, and z components of the velocity vector, embodies this principle [64,70]:

$$\vec{\nabla}\vec{V} = 0 \tag{3.1}$$

This equation illustrates the concept of incompressible flow, a scenario where the density of each fluid constituent remains constant throughout the flow, maintaining an invariable density distribution. This property characterizes the behavior of fluid within this specific context, underlining the incompressibility aspect of the flow.

3.1.1.2. Conservation of Momentum

In fluid dynamics, the conservation of momentum is a fundamental principle that governs the motion of fluids and plays a pivotal role in understanding fluid behavior. It stems from Newton's second law of motion and is particularly important when analyzing the flow of fluids in various contexts, such as in pipelines, rivers, or aerodynamics. The principle dictates that the total momentum of a closed system of fluid particles remains constant as long as no external forces act on the system. This concept enables us to predict how fluid motion changes in response to different conditions, like changes in velocity, pressure, or viscosity. Conservation of momentum forms the basis for studying fluid flow patterns, analyzing the effects of forces on fluid

particles, and predicting the outcomes of fluid interactions. It is a cornerstone in the field of fluid dynamics, providing valuable insights that help engineers and scientists optimize designs, make informed decisions, and comprehend the complex behavior of fluids in various real-world scenarios.

Momentum equation [64,70]:

$$\rho \frac{D\vec{V}}{Dt} = -\Delta P + \mu \nabla^2 \vec{V} \tag{3.2}$$

3.1.1.3. Conservation of Energy

The law of conservation of energy in physics and chemistry asserts that the total energy of an isolated system remains constant over time; this is referred to as being conserved over time. [65] [66] [67]. This concept, first proposed and tested by Emilie du Châtelet [66] [67], states that energy cannot be created or destroyed, but can only be converted or transferred from one form to another. When a stick of dynamite explodes, for example, chemical energy is transformed into kinetic energy. After calculating and summing up all the different types of energy released during the explosion, such as the kinetic energy and potential energy of the pieces, in addition to heat and sound, one can calculate the precise decrease in chemical energy that occurred during the combustion of dynamite.

It logically follows from the law of conservation of energy that a perpetual motion machine of the first kind cannot exist. This means that no system without an external energy source can continuously produce an unlimited quantity of energy to its surrounding environment, which is impossible. [68] The conservation of energy may not be achievable for systems lacking temporal translation symmetry in their design. For instance, consider the curved space times of general relativity [69] or the time crystals observed in condensed matter physics [64,70].

$$\rho c_p \frac{DT}{Dt} = k \nabla^2 T \tag{3.3}$$

3.1.2. Turbulence k-ε (RNG) Model

The k-ε turbulence model is the prevailing choice for simulating mean flow behaviors in computational fluid dynamics (CFD), particularly under turbulent flow conditions. This two-equation model employs a pair of transport equations to provide a comprehensive description of turbulence within the flow. The selection of the RNG (Renormalization Group) variant of this model was motivated by its significant prominence in Ansys-based numerical simulations, as evident in notable works such as [46] and [61]. This model has demonstrated high precision in delivering results, particularly in handling turbulent flow scenarios, making it a favored choice in numerical heat transfer simulations.

The distinguishing feature of the RNG k-epsilon model lies in its incorporation of swirl effects on turbulence, resulting in improved accuracy for swirling flows. Furthermore, when dealing with turbulent Prandtl numbers, the RNG model offers an analytical formulation, as opposed to the standard k-model, which relies on fixed user-specified values. Notably, the RNG model extends its applicability beyond High-Reynolds number scenarios by providing an analytically-derived formulation for effective viscosity, accounting for Low-Reynolds number effects—a feature not present in the standard k-model.

However, it's essential to note that the effectiveness of this feature in the RNG k-model hinges on the proper treatment of the near-wall region. When executed correctly, the RNG k-model outperforms the standard k-model, offering enhanced accuracy and reliability across a broader spectrum of flow scenarios. This makes the RNG k-epsilon turbulence model an invaluable tool for a wide range of flow simulations, particularly when capturing intricate turbulence effects and addressing Reynolds number considerations.

Renormalization Group (RNG) methods play a crucial role in the development of the RNG-based k-turbulence model. This process begins by starting with the instantaneous Navier-Stokes equations, which serve as the foundation for deriving the k-turbulence

model. Unlike the standard k-model, the RNG-based approach involves an analytical derivation that introduces several distinctions.

In this newly formulated model, the constants utilized differ from those in the standard k-model. Additionally, the diffusion equation for both ε (dissipation rate of turbulence kinetic energy) and k (turbulence kinetic energy) incorporates new terms and functions. These modifications are essential for capturing a more accurate representation of turbulence behavior and improving the model's overall performance in diverse flow scenarios.

For a comprehensive understanding of the RNG theory and its practical application to turbulence modeling, detailed information can be found in reference [70]. This source provides in-depth insights into the theoretical underpinnings of RNG, its methodologies, and the specific advancements it brings to the field of turbulence modeling, shedding light on the nuances that make the RNG-based k-turbulence model a valuable tool for simulating complex turbulent flows [64,70].

$$\frac{\partial}{\partial t}(\rho k) + \frac{\partial}{\partial x_i}(\rho k u_i) = \frac{\partial}{\partial x_i}\left(\alpha_k \mu_{eff} \frac{\partial k}{\partial x_j}\right) + G_b + G_k - Y_M - \rho\varepsilon + S_k \tag{3.4}$$

$$\frac{\partial}{\partial t}(\rho \epsilon) + \frac{\partial}{\partial x_i}(\rho \epsilon u_i) = \frac{\partial}{\partial x_j}\left(\alpha_\epsilon \mu_{eff} \frac{\partial \epsilon}{\partial x_j}\right) + C_{1\epsilon}\frac{\epsilon}{k}(C_{3\epsilon}G_b + G_k) - C_{2\epsilon}\rho\frac{\epsilon^2}{k} - R_\epsilon + S_\epsilon \tag{3.5}$$

G_k represents the generation of turbulence kinetic energy due to mean velocity gradients, G_b is the generation of turbulence kinetic energy due to buoyancy, and Y_M represents the contribution of fluctuating dilatation in incompressible turbulence to the overall dissipation rate [64,70].

$C_{1\,\varepsilon} = 1.42$ and $C_{2\,\varepsilon} = 1.68$ (constants) (3.6)

$\alpha_k = 1$ and $\alpha_\varepsilon = 1$ (turbulent Prandtl numbers for k and ε) (3.7)

The flow velocity components parallel and perpendicular to the gravitational vector are represented by v and u, respectively. Consequently, for buoyant shear layers aligned with the direction of gravity, $C_{3\varepsilon}$ becomes 1. For buoyant shear layers' perpendicular to the gravitational vector, $C_{3\varepsilon}$ becomes 0.

$$C_{3\varepsilon} = \tanh\left|\frac{v}{u}\right| \tag{3.8}$$

When comparing the RNG and standard k- models, the most significant difference is the inclusion of an additional term in the ε equation [64,70]:

$$R_{\varepsilon} = \frac{C_{\mu}\rho\eta^{3}\left(1-\frac{\eta}{\eta}\right)\varepsilon^{2}}{1+\beta\eta^{3}\qquad k} \tag{3.9}$$

$$\boldsymbol{\eta}_{\circ} = 4.38 \quad , \quad \boldsymbol{\beta} = 0.012 \ , \boldsymbol{\eta} = \mathrm{SK}/\,\varepsilon \tag{3.10}$$

3.2.PARAMETERS AFFECTING HEAT EXCHANGERS

3.2.1. Pressure Drop

The term "pressure drop" describes the variance in pressure between two points within a fluid-conveying system. This decrease in pressure arises when the fluid encounters resistance during its passage through the conduit, primarily due to frictional forces. Whenever fluid traverses a pipe, a pressure drop arises due to this resistance to flow. Additionally, variations in elevation between the pipe's inlet and outlet points can result in either a pressure increase or a decrease. Several factors contribute to the overall pressure disparity across the pipe. Notably, frictional loss arises as fluid encounters pipe fittings, bends, valves, or other components, causing friction between the fluid and the pipe walls. This pressure loss or drop can also be attributed to the elevation change of the fluid, especially in cases where the pipe is not horizontal. The formula that governs pressure drop is provided as [64,70]:

$$\Delta P = f\frac{L}{D}\frac{\rho V^{2}}{2} \tag{3.11}$$

The pressure drop (ΔP) in Pascal's (Pa) within a tube can be calculated using various factors, including the friction factor (f), the length of the tube (L) in meters (m), the velocity of the fluid (v) in meters per second (m/s), the density of the fluid (ρ) in kilograms per cubic meter (kg/m³), and the inner diameter of the tube (D) in meters (m).

3.2.2. Mean Temperature

To find the fluid properties on each side of a heat exchanger, the mean (flow length average) temperature is determined for each fluid. Essential fluid parameters for pressure drop and heat transfer calculations include density, viscosity, specific heat, thermal conductivity, and Prandtl number. An essential factor to consider is the assumption of homogeneity in fluid/solid thermophysical characteristics, which is a fundamental aspect of heat exchanger design theory. The temperatures at which fluid qualities should be evaluated are referred to as fluid mean temperatures [64,70].

$$T_{average} = (T_{inlet} + T_{outlet}) / 2 \quad (3.12)$$

3.2.3. Mean Velocity

Due to the no-slip condition, the fluid velocity within a duct can range from zero at the surface to a maximum at the middle of the duct. As a result, when working with a fixed cross-sectional area for the duct, it's more practical to utilize an average or mean velocity denoted as V_m. This mean velocity remains constant for incompressible fluid flow, ensuring a steady reference point. When applying the principle of conservation of mass to the duct, it becomes possible to derive the value of the mean velocity V_m as outlined in the following manner [64,70]:

$$\dot{m} = \rho V_m A_c \quad (3.13)$$

where ρ representing the fluid's density in kg/m³, m denoting the mass flow rate of the fluid in kilograms (kg), A_c the cross-sectional area of the duct in square meters (m²),

and V_m stands for the mean velocity of the fluid within the duct in meters per second (m/s).

For incompressible fluid flow in a duct, the mean velocity can be expressed as follows [64,70].:

$$V_m = \frac{\dot{m}}{\rho A_c} \tag{3.14}$$

3.3. DIMENSIONLESS NUMBERS

In engineering analysis and design, dimensionless numbers are frequently connected with certain performance metrics and are quite useful. The Nusselt number (Nu), the Reynolds number (Re), and the Darcy friction factor (f) are only a few of the dimensionless numbers used in forced convective heat transfer.

3.3.1. Reynolds Number (Re)

A dimensionless value, the Reynolds number aids in predicting flow patterns across various fluid flow scenarios. Laminar (layer-like) flow typically dominates in cases of low Reynolds numbers, while turbulent flow tends to prevail in scenarios with higher Reynolds numbers. Turbulent flow emerges due to variations in fluid speed and direction, occasionally resulting in collisions or even flow directions opposite to the main stream (referred to as eddy currents). These eddy currents, along with flow fluctuations, consume energy and thereby increase the likelihood of cavitation within a liquid. In fluid mechanics, Reynolds numbers, being dimensionless quantities, play a crucial role. They represent the ratio of inertia forces to viscous forces within a fluid [64,70].

$$Re = \frac{\rho V D_h}{\mu} = \frac{V D_h}{\nu} \tag{3.15}$$

where ν represents flow velocity (m/s), ρ signifies density (kg/m³), μ represents dynamic viscosity (N.s/m²), D stands for hydraulic diameter or characteristic linear dimension (m), and ν denotes kinematic viscosity (m²/s).

3.3.2. Nusselt Number (Nu)

The Nusselt number, a dimensionless quantity closely connected to the Péclet number, serves as a critical parameter in thermal analysis. Both numbers play a role in expressing the ratio of convective thermal energy to the thermal energy transmitted within the fluid, and their applications are analogous. The Nusselt number essentially represents the dimensionless temperature gradient at the surface and acts as a metric for quantifying the convective heat transfer transpiring at that surface [64]. The origins of the Nusselt number are attributed to a German engineer named Wilhelm Nusselt. This concept arises when the conductive component is evaluated under conditions involving stagnant fluid rather than a flowing fluid, providing a direct relationship between convective and conductive heat transfer across a surface [64,70].

$$Nu = \frac{\mathrm{hD_h}}{\mathrm{K}} \tag{3.16}$$

where K represents thermal conductivity of the fluid (W/m.K), D is the hydraulic diameter (m), and h stands the convective heat transfer coefficient (W/m^2.K).

3.3.3. Darcy Friction Factor

The Darcy friction factor, a dimensionless value, plays a crucial role in the Darcy–Weisbach equation, which characterizes frictional losses in pipes, ducts, and open-channel flow. This factor is known by various names, such as the Darcy–Weisbach friction factor, friction factor, or resistance coefficient. The Darcy–Weisbach equation can be expressed in two distinct forms: the head loss form and the pressure loss form. Below, we present a formalized paraphrase of the head loss form as an illustrative example [64,70].

$$\frac{\Delta h}{L} = f_D . \frac{1}{2g} . \frac{V^2}{D} \tag{3.17}$$

In the pressure loss form, the Darcy–Weisbach equation can be expressed as[64,70]:

$$\frac{\Delta P}{L} = f_D . \frac{\rho}{2} . \frac{V^2}{D} \quad (3.18)$$

where ΔP shows the pressure loss due to friction (Pa), L is the pipe length (m), f_D is the Darcy friction factor, D is the hydraulic diameter of the pipe (m), V is the mean flow velocity V (m/s), ρ is the density of the fluid (kg/m^3). Δh represents the head loss resulting from friction (m), while the gravitational constant is g (m/s²).

3.3.4. Prandtl Number

According to the definition given by Ludwig Prandtl, the Prandtl number (Pr) or Prandtl group is a dimensionless number named after the German physicist Ludwig Prandtl, which is defined as the ratio of momentum diffusivity to heat diffusivity [71]. Formal paraphrase formal phrasing according to the data, the Prandtl number is:

$$Pr = \frac{\upsilon}{\alpha} = \frac{C_p \mu}{k} \quad (3.19)$$

where ν represents kinematic viscosity (m^2/s), α is thermal diffusivity (m^2/s), μ is dynamic viscosity (N.s/m^2), k is thermal conductivity (W/m.K), c_p is specific heat (J/kg.K), and ρ is density (kg/m^3) .

3.4. NUMERICAL MODELING

3.4.1. Physical Model

The physical model used in the thesis was created using the SolidWorks program. This model was then imported into the Ansys program for simulation purposes. The tube and twisted tape had fixed lengths of 1000 mm in all cases. The tube's inner diameter was D_i = 17 mm, and the outer diameter was D_o = 21 mm as shown in Figure 3.1 and 3.2. The diameter of the holes and dimples was 8 mm. The twisted tape possessed a thickness of 1 mm and a width of 17 mm, as illustrated in the Figure 3.3. Water served as the working fluid in the simulation process, and Stainless Steel 304 was employed for constructing the tube and twisted tapes.

In the case of the twisted tape, the pitch is defined as the distance between two points on the same plane, measured along the tape's axis. The twist ratio, denoted as "y" is calculated by dividing the twist pitch length by the tape width (y = H/w). The pitch length for the twisted tape was uniformly set at 100 mm, resulting in a constant twist ratio of (y = 5.88) for all tape configurations (Figure 3.3). The perforated (P_P) and dimpled (P_d) tapes featured three distinct hole pitch lengths, namely (25, 50, 100) mm (Figure 3.4-3.6). The hole pitch ratios (P_p/H) and (P_d/H) were (0.25, 0.5, 1).

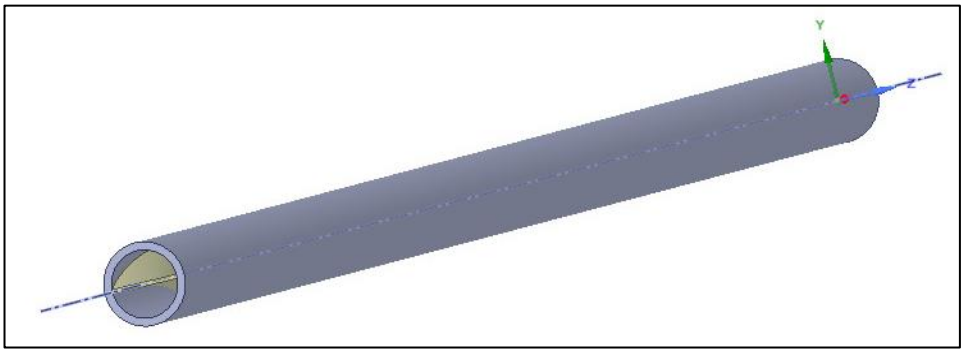

Figure 3.1. Geometry of twisted tape inserted tube.

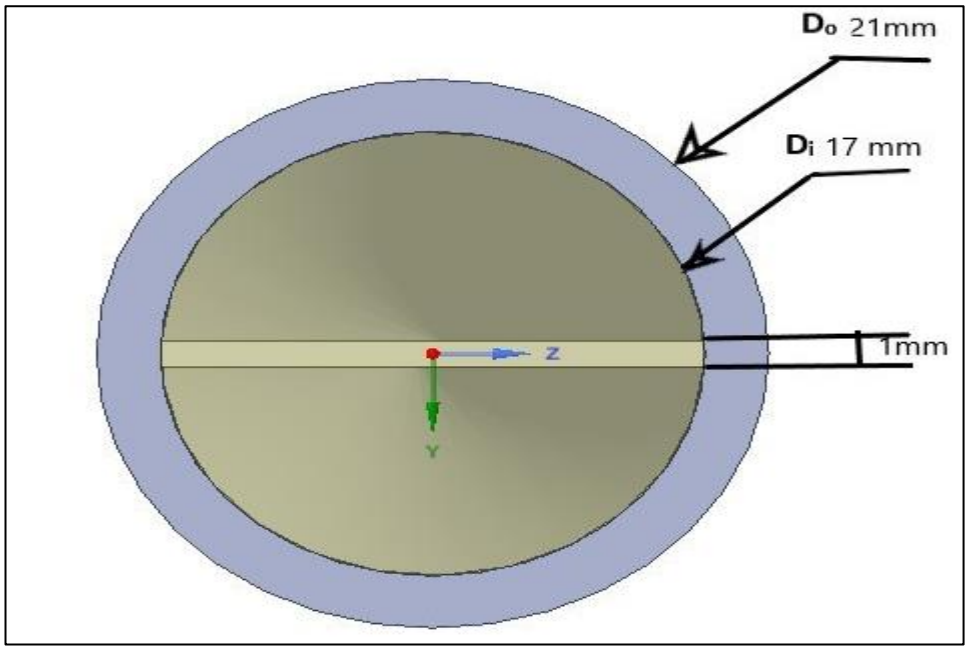

Figure 3.2. Dimensions of the twisted tape inserted tube from the cross-section view.

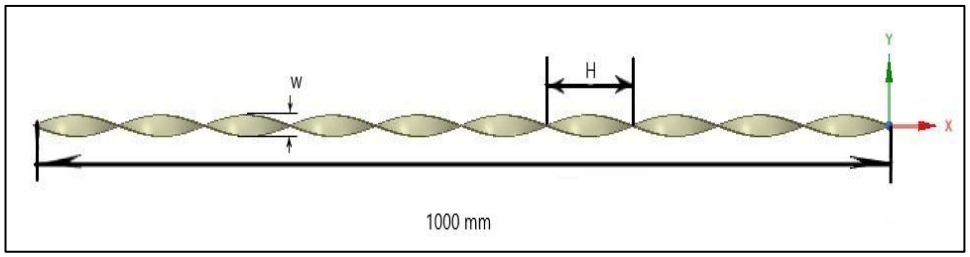

Figure 3.3. Geometry of the plain twisted tapes.

The physical model of the plain twisted tape was drawn, and then circular holes with a diameter of 8 mm were drawn equally distributed along the length of the twisted tape. The distance between the center of the first hole and the center of the second hole is called hole pitch length perforated and symbolized by (P_p), which is of three different lengths: 25, 50, 100 mm as shown in Figure 3.4.

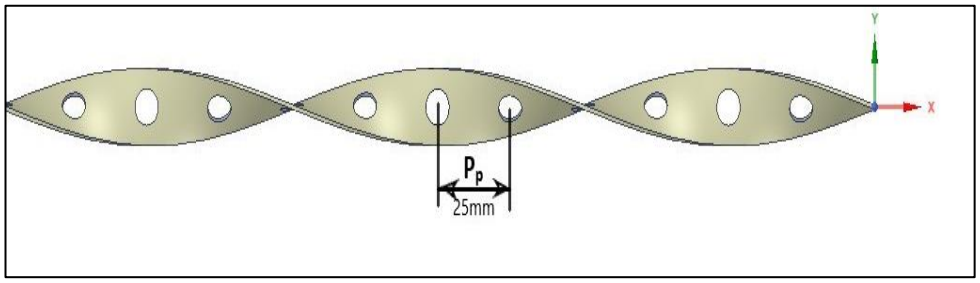

Figure 3.4. Geometry of the perforated twisted tapes.

The physical model of the plain twisted tape was drawn, and then the dimples were drawn with a diameter of 8 mm and a height of 4 mm distributed evenly along the length of the twisted tape (Figure 3.5). The distance between the center of the first dimple and the center of the second dimple is called the pitch dimple length, symbolized by (P_d), and it has three different lengths: 25, 50, 100 mm as shown in the Figure 3.5.

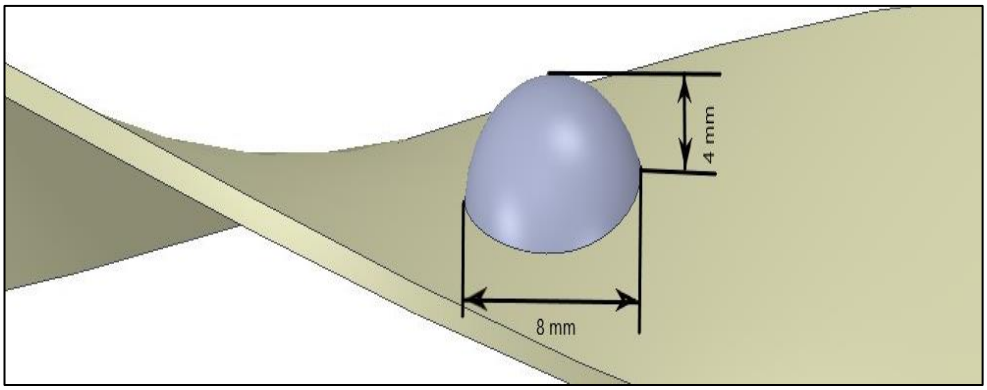

Figure 3.5. Dimensions of the dimples on twisted tapes.

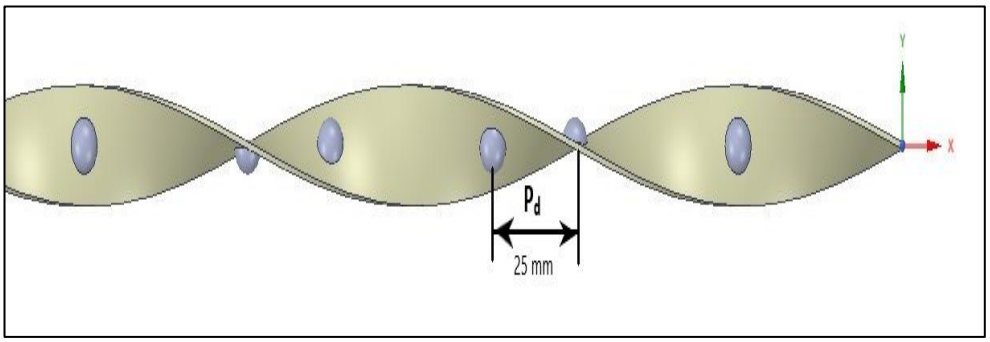

Figure 3.6. Geometry of the dimpled twisted tapes.

Table 3.1. Summary drawn twisted tape configurations.

Configuration	Y [mm]	w [mm]	Y / w	P_p [mm]	P_d [mm]	P_p / Y	P_d / y
Plain TT	100	17	5.88				
Perforated	100	17	5.88	25		0.25	
TT	100	17	5.88	50		0.5	
	100	17	5.88	100		1.0	
Dimpled TT	100	17	5.88		25		0.25
	100	17	5.88		50		0.5
	100	17	5.88		100		1.0

3.4.2. Boundary Conditions

The calculations in this study were conducted using the commercial ANSYS Fluent computational fluid dynamics (CFD) code. The setup and boundary conditions were defined as follows: the solver type was set to pressure-based, and steady-state. RNG k-ε model Enhanced Wall Function was chosen as the viscous turbulence model for

tubes with inserted twisted tape, because it is widely reached that this turbulence model gives better results compared to others [1]. A constant heat flux value of 10000 W/m² was applied to all walls. In all cases, the fluid inlet temperature was maintained at a fixed value of 300 K. To obtain the pressure gradient, a specified mass flow rate was input into the code. This pressure gradient value was essential for the subsequent friction factor calculations. Water, with constant properties, served as the working fluid throughout the simulations. SIMPLE scheme is used for Pressure-Velocity coupling and 2nd order upwind is used for pressure, momentum, turbulent kinetic energy, turbulent dissipation rate, and energy discretization.

In this study, the focus was on enhancing the turbulent flow thermal performance of the twisted tape (TT), as turbulent flow generally provides better heat transfer compared to laminar flow. The unique geometries of dimples and protrusions on a twisted tape make its characteristics challenging to predict. As a result, the study covered a range of Reynolds numbers, specifically in the range of 10000-20000, to gain a comprehensive understanding of the behavior.

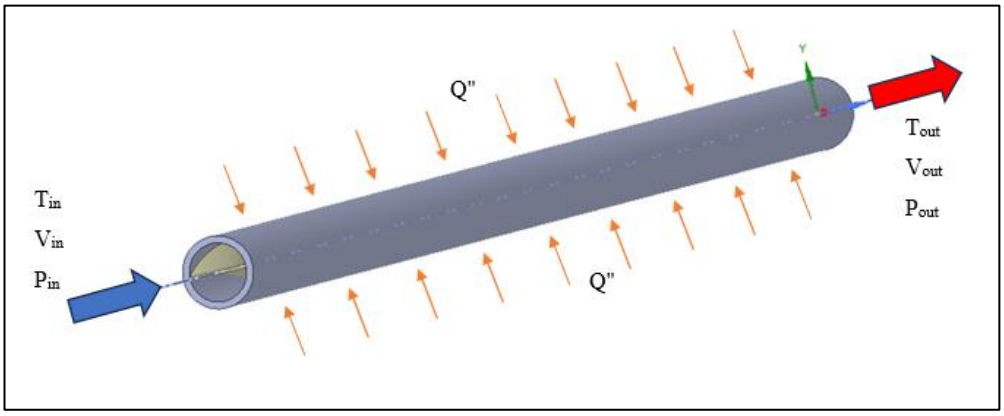

Figure 3.7. Boundary conditions of the problem geometry.

3.4.3. Grid-Independence Test

The selected mesh type utilized in this study is the tetrahedral mesh, comprising triangular shapes. This mesh configuration, as depicted in Figure 3.8-3.10, effectively fills all gaps with elements of consistent size, contributing to a faster solution process due to the uniform symmetry between the cells. As can be seen

from the figures, inflation layers were created to simulate the boundary layer more precisely. Hence, denser mesh was created near proximity and curvatures.

In order to obtain accurate results, meshes were created for a range of grid cell counts, including the minimum of 68,000 cells and the maximum of 2,160,000 cells. After the analyses, the mesh consisting of 352,000 cells was determined to be the optimal choice, offering the best compromise between accuracy and computational efficiency. Through this mesh, various parameters were derived, including the outlet temperature of the water, wall temperature, velocity, and pressure.

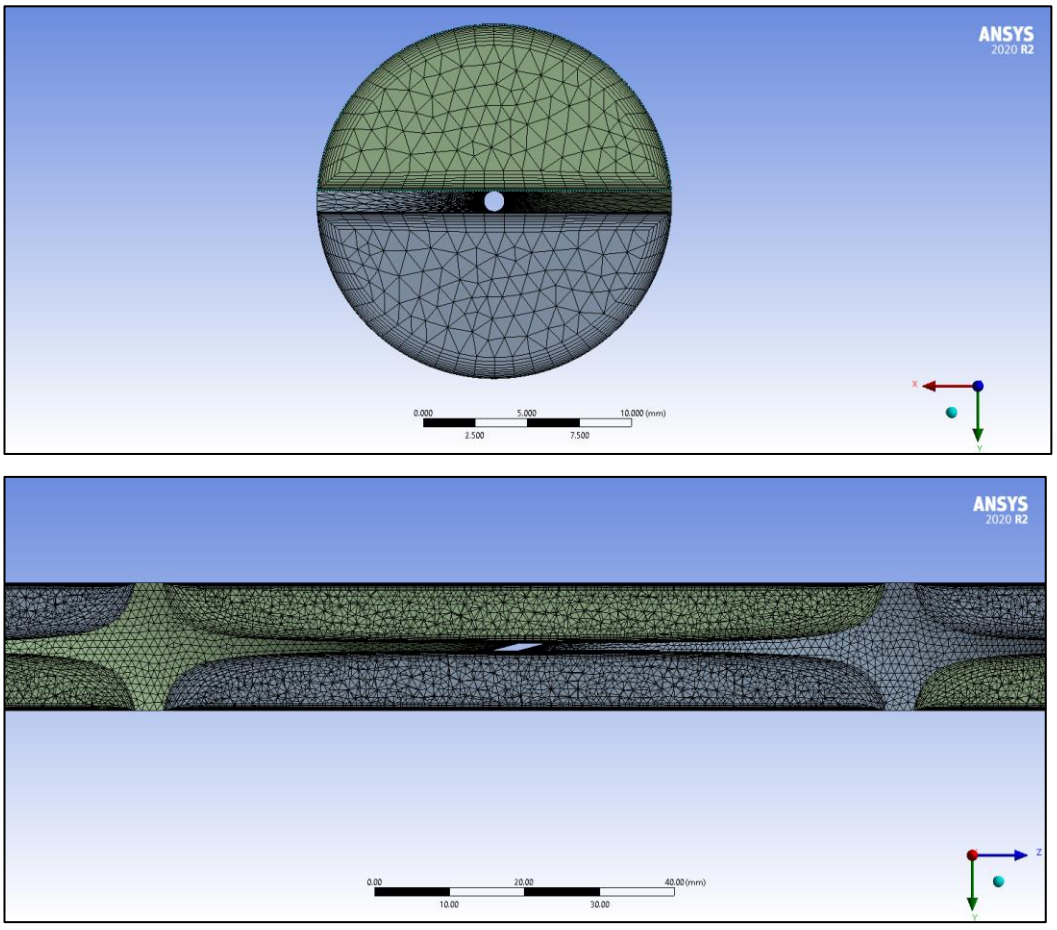

Figure 3.8. Mesh distribution of plain twisted tape inserted tube.

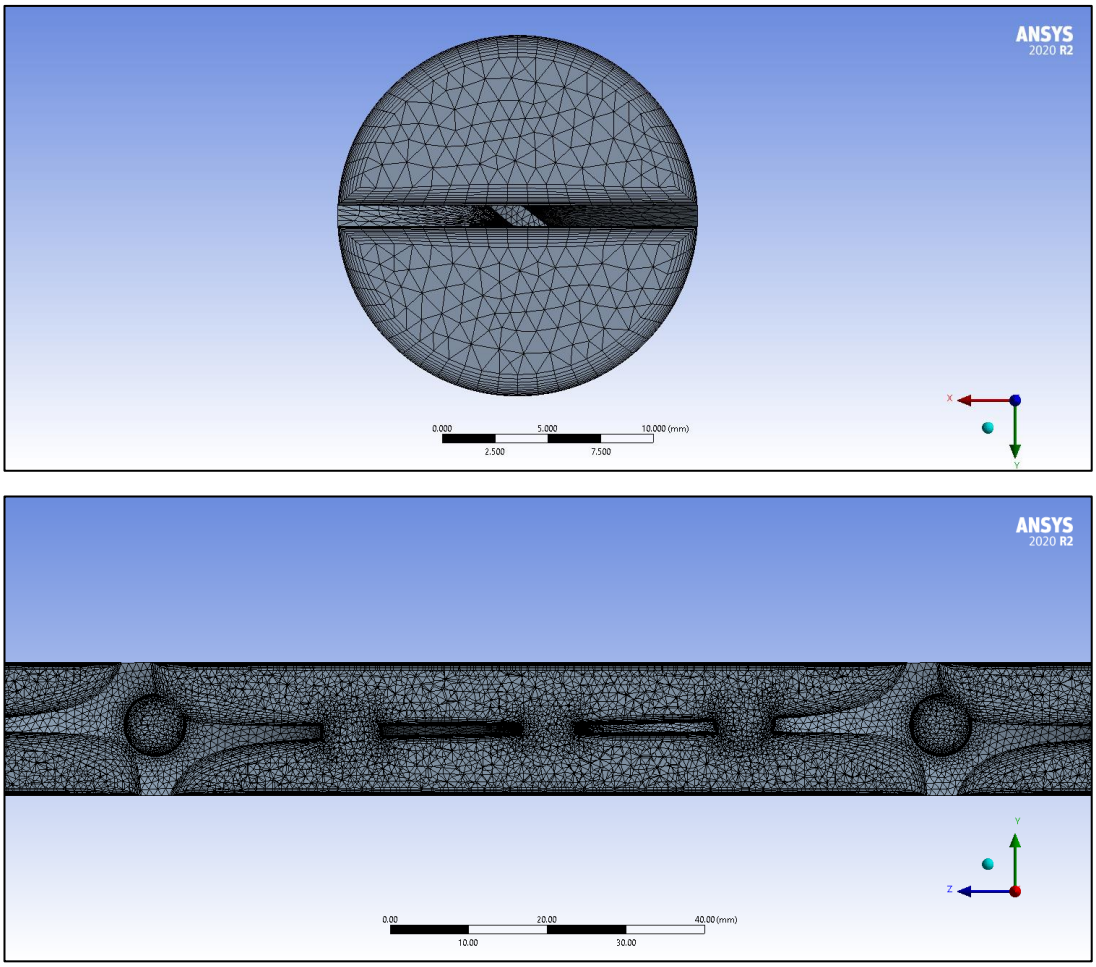

Figure 3.9. Mesh distribution of perforated twisted tape inserted tube.

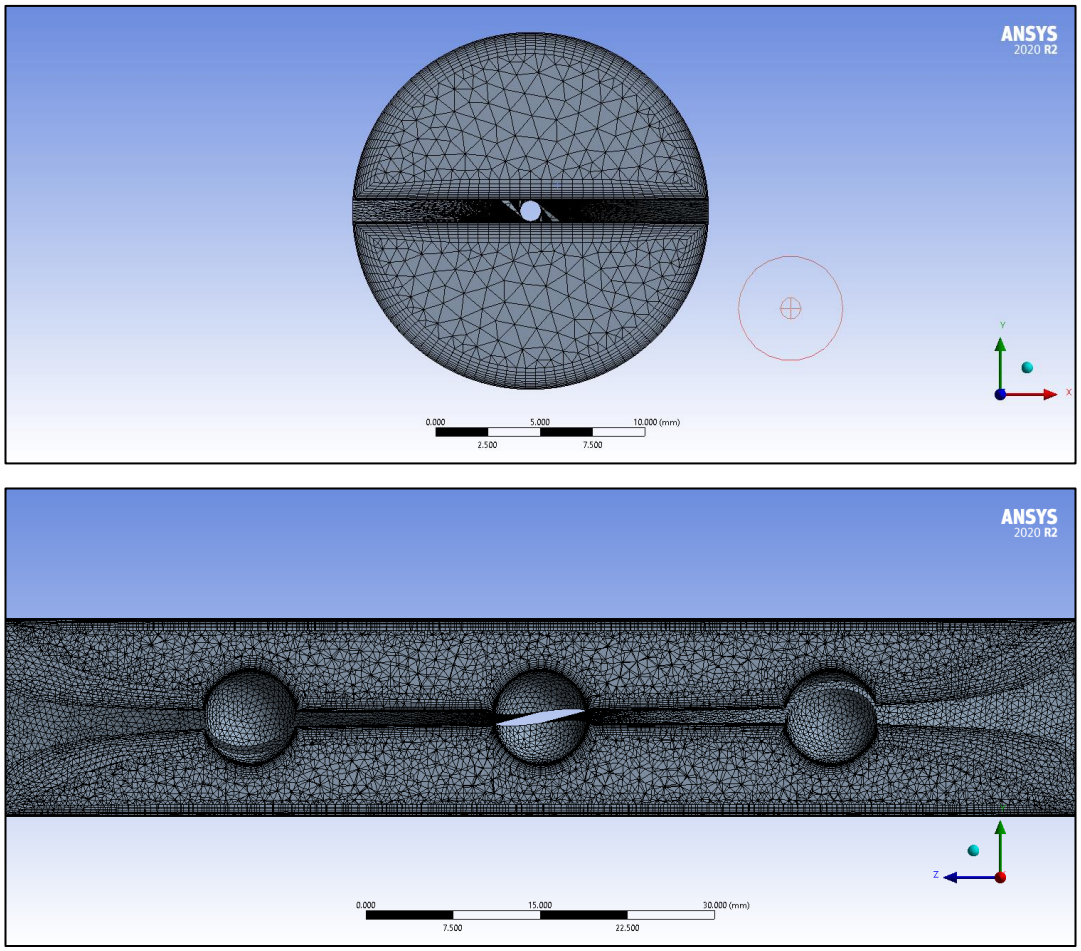

Figure 3.10. Mesh distribution of dimpled twisted tape inserted tube.

Figure 3.11 shows the graphical relationship between the mesh number with the Nusselt number and friction factor values, where the plain tape was chosen as the original state of the tapes. An convergence was noticed in the Nusselt value with the increase in the number of meshes until it reaches the number of meshes (2,160,000), where it is noted that there is a convergence of the Nusselt value around the number of meshes (352,000), and these values are close to stability. Therefore, the meshing method of (352,000) was adopted to simulate the rest of the twisted tapes.

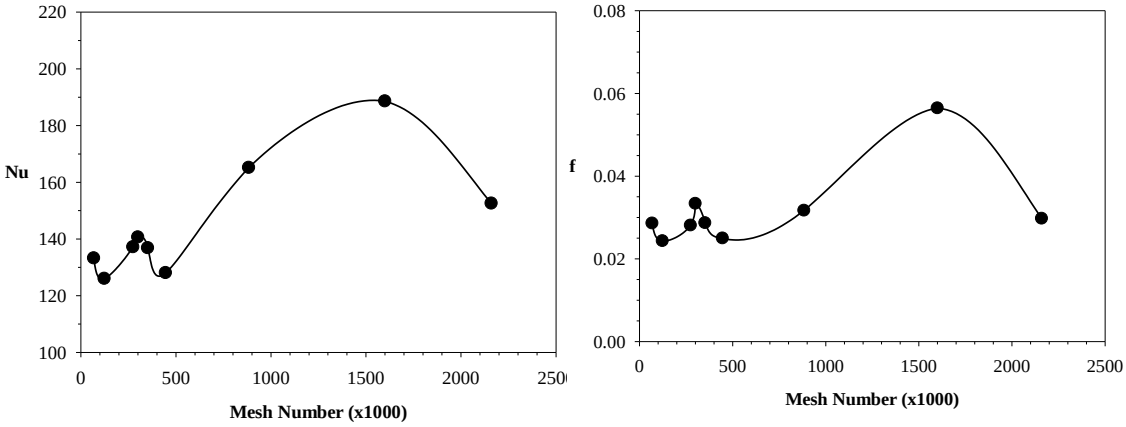

(a) (b)

Figure 3.11. Variation of a) Nusselt number and b) friction factor with mesh number.

PART 4

RESULTS AND DISCUSSION

In this chapter, the results obtained from the numerical analyses of the tubes including smooth tube, plain twisted tape inserted tube, perforated twisted tape and dimpled twisted tape inserted tubes using water as working fluid were discussed. Perforated twisted tapes are created by making holes in the twisted tape with a diameter of 8 mm and at different distances 25, 50, and 100 mm. Dimpled twisted tapes are created by adding the shape of a hemisphere with an 8 mm diameter at different distances 25, 50, 100 mm. These eight cases are discussed below and shown in the following figures. Also, the contours of temperature, velocity, and pressure of the seven cases are discussed at Figure 4.6 - 4.12.

Firstly, obtained numerical results are compared with the literature in Figure 4.1. The error margin of ±4.28% is obtained for Nu values according to the Dittus-Boelter correlation and ±2.26% according to [20]. Also, the error margin of ±5.62% is obtained for the friction factor compared to Darcy-Weisbach equation and ±1.63% compared to [20].

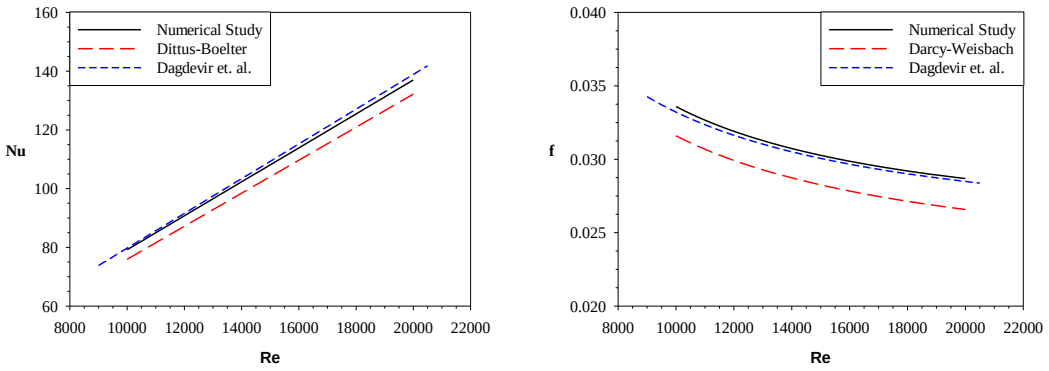

(a) (b)

Figure 4.1. Validation of obtained numerical results with literature.

Furthermore, further comparisons for twisted tape inserted tubes can be found in Figure 4.2. For perforated twisted tape inserted tubes, the error margin of ±5.31% is obtained and ±10.53% for dimpled twisted tape inserted tubes according to [20]. These results show that the numerical analyses are in good agreement with the literature.

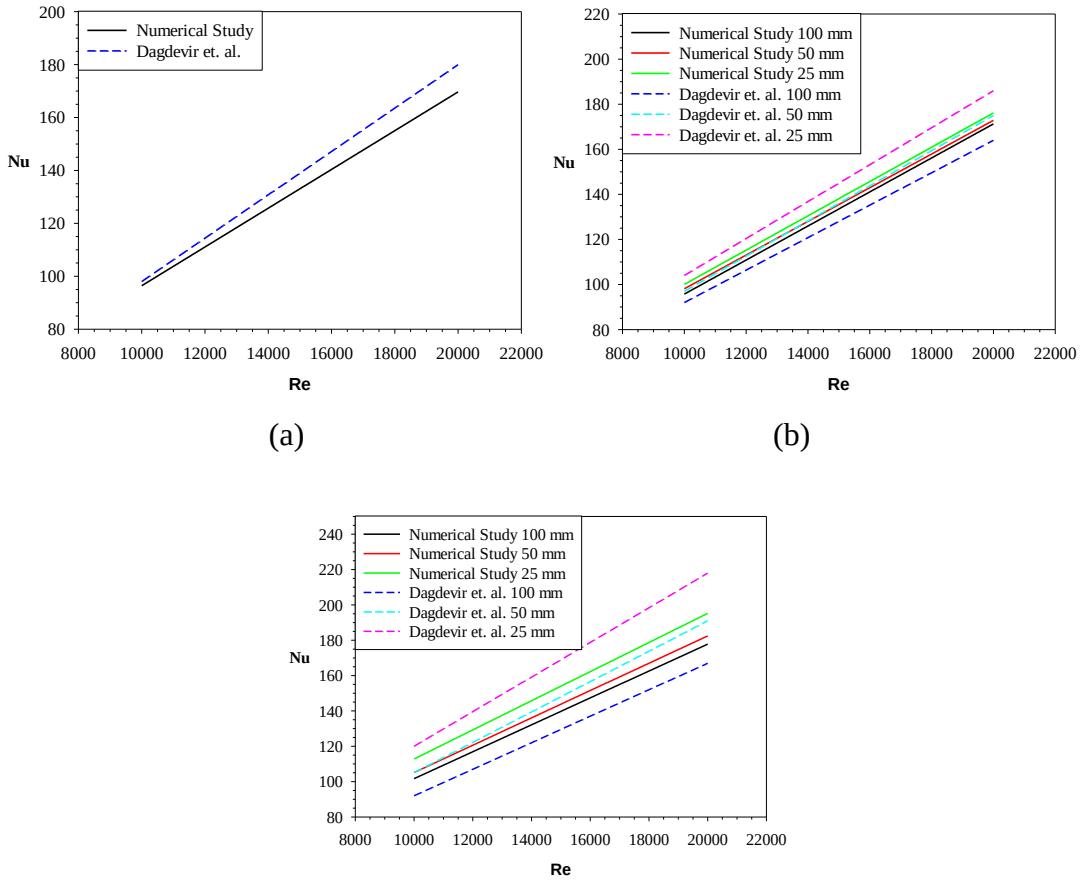

Figure 4.2. Comparison of numerical results consisting a) plain twisted tape, b) perforated twisted tape, and c) dimpled twisted tape inserted tubes with literature.

As can be seen in Figure 4.3, plain twisted tape contributes up to 24% more heat transfer rate compared to smooth tube. This result is excepted due to increase of heat transfer surface and vorticity which disrupts the thermal boundary layer more. On the other hand, perforated twisted tapes increases the convective heat transfer rate up to 28.7%. Decrease of the distance between perforations increases Nusselt number. Perforated twisted tape inserted tube with 100 mm distance has negligible effect on

heat transfer compared to plain twisted tape inserted tube as can be seen in the figure. Local vortexes created by these perforations can increase the Nusselt number, but also these can impact the friction factor. Thus, dimpled twisted tape inserted tubes presented best thermal performance among all the cases. Again, with the increase in the distance between dimples contribute higher heat transfer rates. Best case is obtained in the case of dimples twisted tape inserted tube with 25 mm distance with 42% increase in thermal performance. As dimples increase the heat transfer surface and create disturbances in the flow, heat transfer enhancements occur.

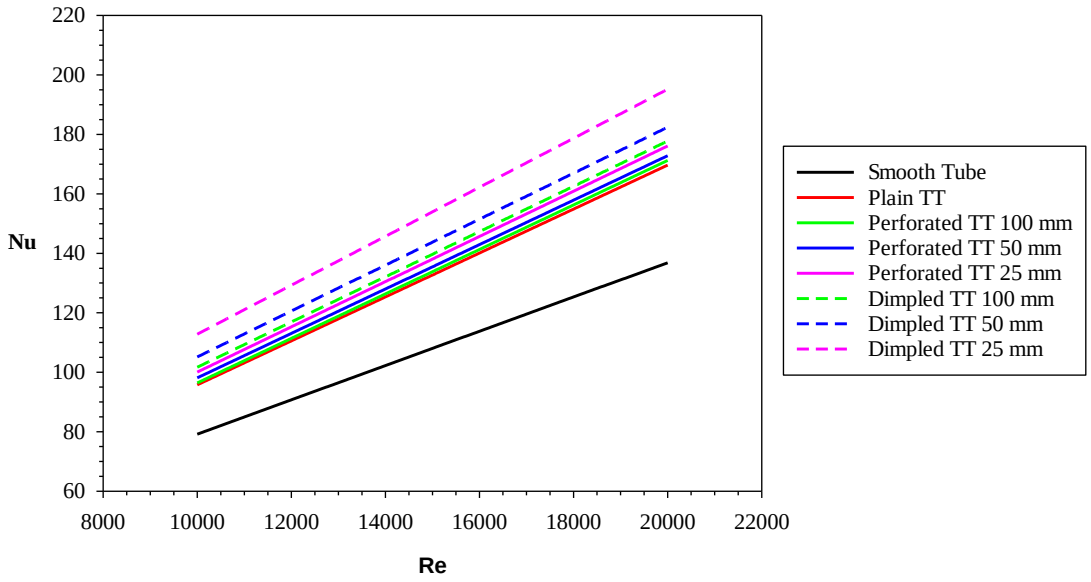

Figure 4.3. Variation of Nusselt number results with Reynolds number.

While twisted tape inserts contribute to higher heat transfer rates, they increase the pressure drop drastically. As can be seen in Figure 4.4, friction factor using plain twisted tape increases up to 1.3 times of smooth tube. Both increasing of surface and vorticity due to twisted tape and dimples cause higher friction factor values.

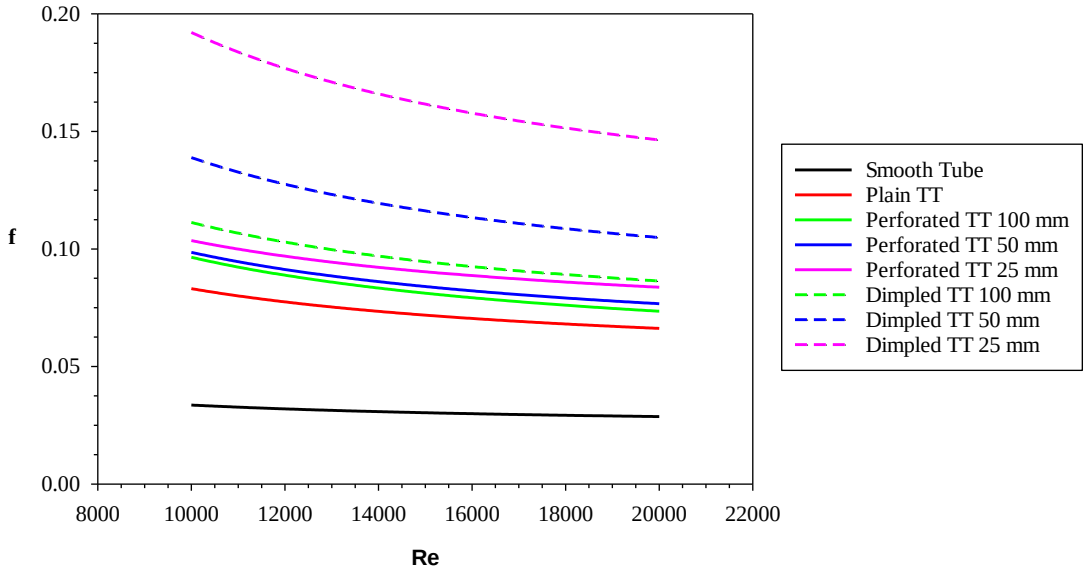

Figure 4.4. Variation of friction factor results with Reynolds number.

This increase in friction factor also affects the performance evaluation criteria of twisted tape inserted tubes as seen in Figure 4.5. Due to higher pressure drop, twisted tapes contribute to efficiency negatively. Furthermore, perforations and dimples cause even lower efficiency. Perforations in the twisted tube cause local vortexes and disturb the flow, so these increases friction factor. Also, dimple fins with increased surface area cause more disturbances and even further increases the friction factor. All these phenomena cause lower performance evaluation criteria even though contributes higher thermal performances.

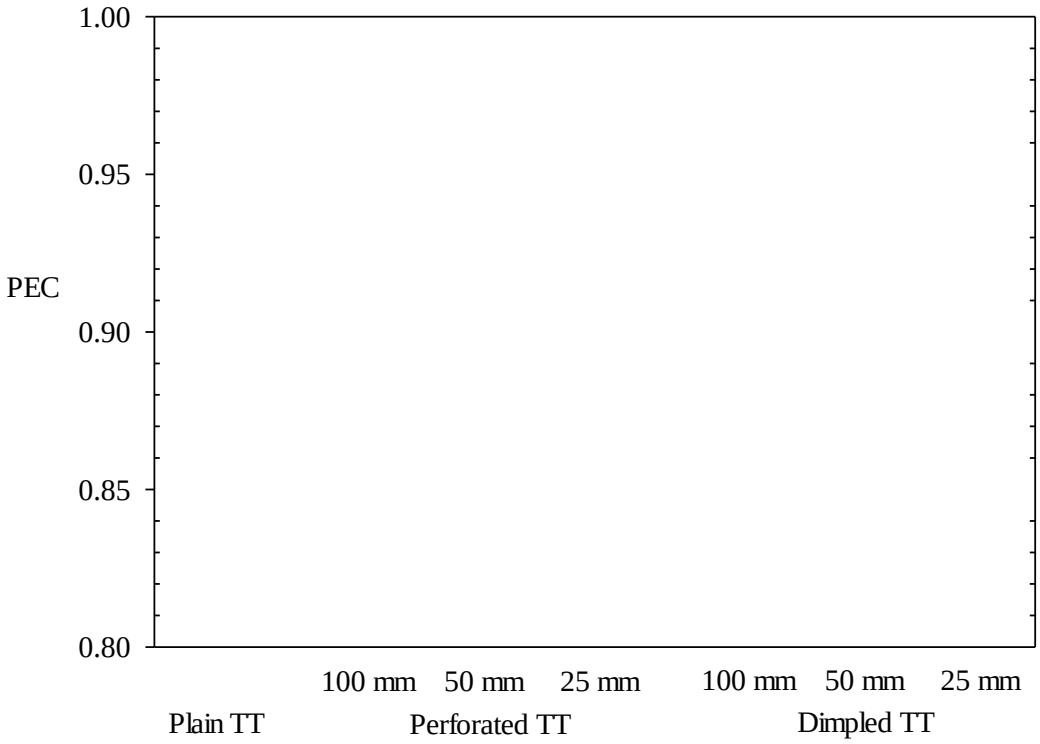

Figure 4.5. PEC values of the cases compared to smooth tube.

From the pressure contours in the inlet section clearly shows that perforations and dimple fins contributes to higher pressure drops across the tube as can be seen in Figure 4.6. Furthermore, as distance between the perforations or dimples decreases, pressure drop increases. This increase is seen more clearly in dimple twisted tape inserted tubes.

Figure 4.7. shows the velocity contours in the outlet section through the seven cases. It is stated that perforations and dimples contribute to higher distribution of maximum velocity among the tube cross-section. This can be attributed to lower boundary layer thickness due to flow disturbances caused by the perforations and dimples. This is also spotted in Figure 4.8. Perforations and dimples cause more homogenous distribution of velocity across the cross-section plain of the tube. In the plain twisted tape inserted tube, the velocity at the center of the half part is more focused; while in perforated twisted tape inserted tubes, it is more distributed. In the dimpled twisted tape inserted tubes, local velocity magnitudes are higher due to increased surface area of dimples and decreased cross section area at the locations of dimples.

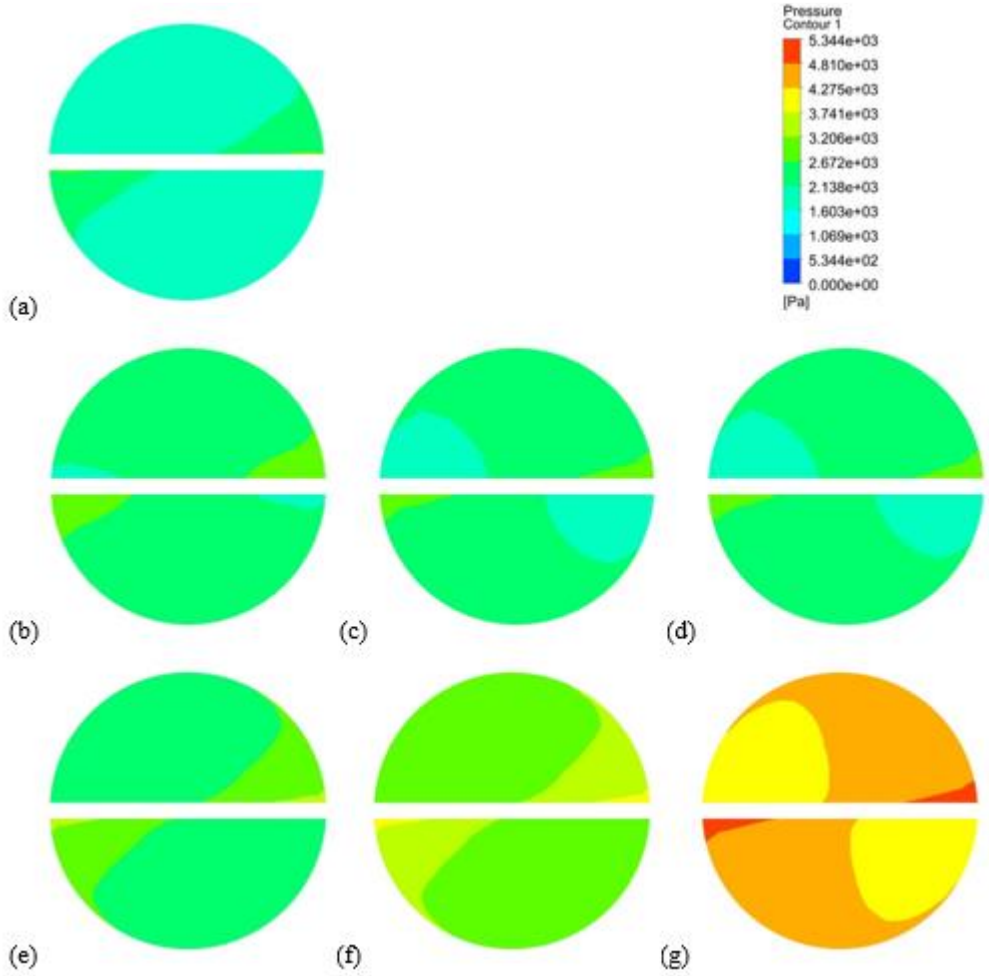

Figure 4.6. Pressure contours of a) Plain TT, b) Perforated TT 100 mm, c) Perforated TT 50 mm, d) Perforated TT 25 mm, e) Dimpled TT 100 mm, f) Dimpled TT 50 mm, g) Dimpled TT 25 mm inserted tubes at outlet section for Re=20000.

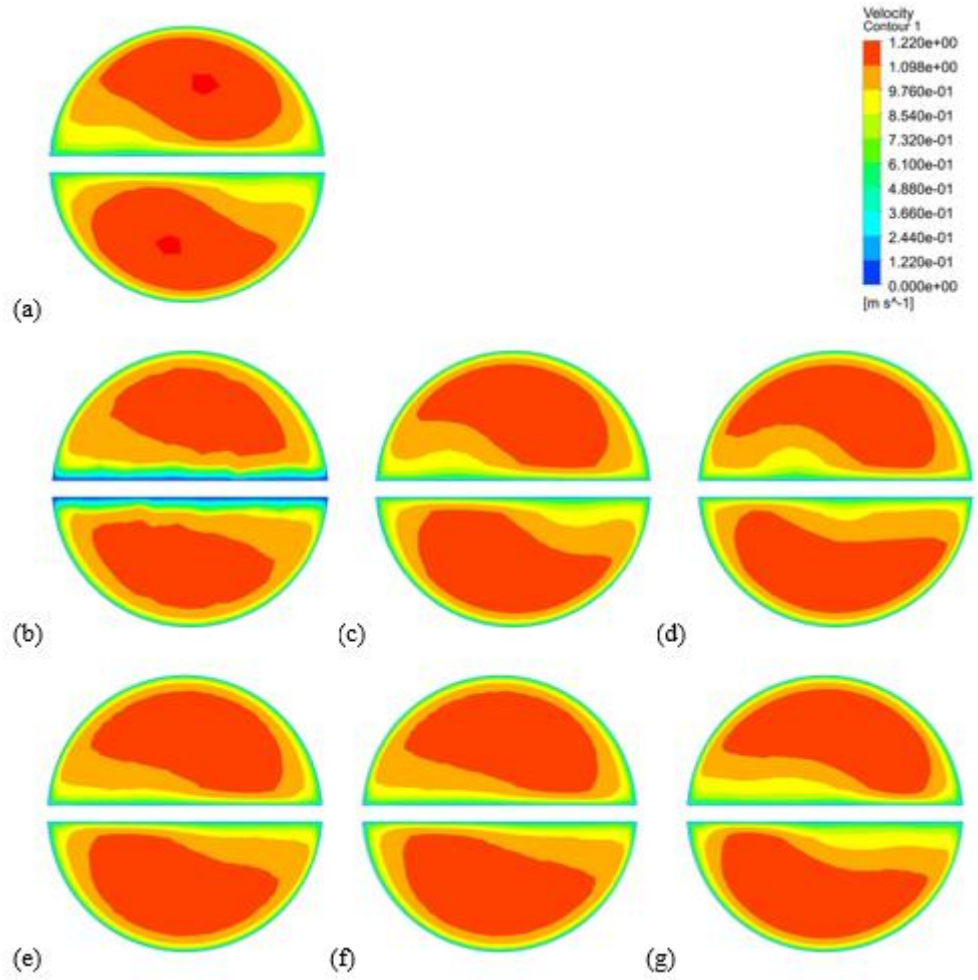

Figure 4.7. Velocity contours of a) Plain TT, b) Perforated TT 100 mm, c) Perforated TT 50 mm, d) Perforated TT 25 mm, e) Dimpled TT 100 mm, f) Dimpled TT 50 mm, g) Dimpled TT 25 mm inserted tubes at outlet section for Re=20000.

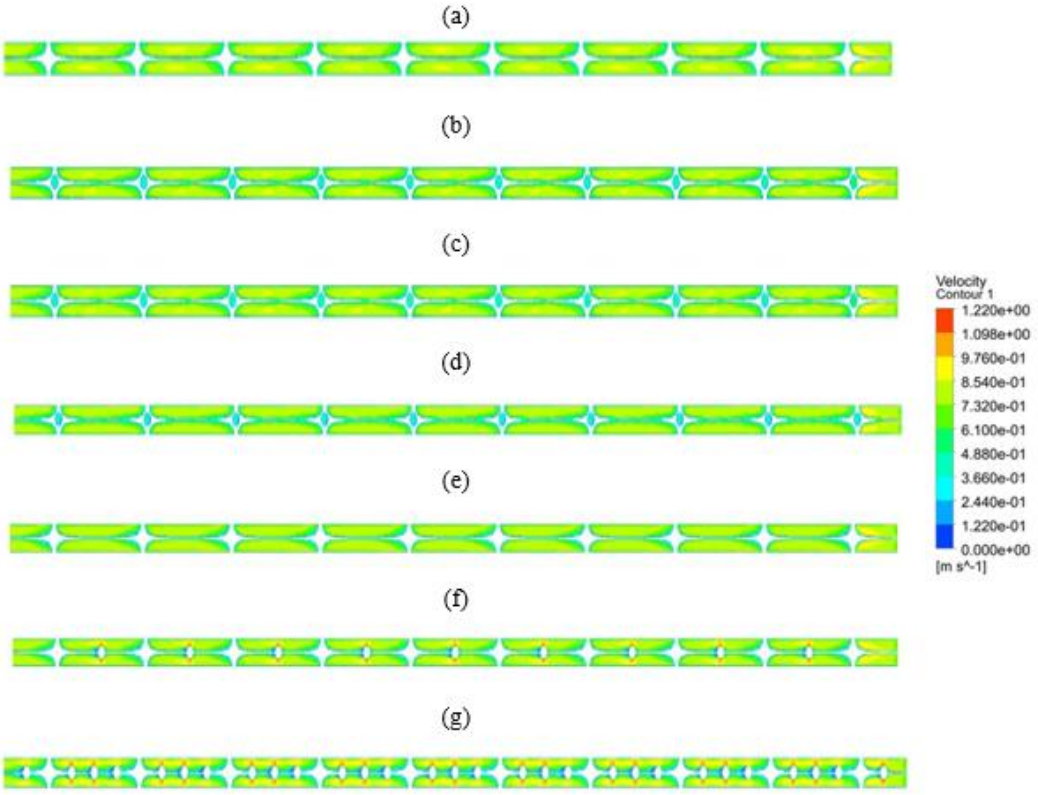

Figure 4.8. Velocity contours of a) Plain TT, b) Perforated TT 100 mm, c) Perforated TT 50 mm, d) Perforated TT 25 mm, e) Dimpled TT 100 mm, f) Dimpled TT 50 mm, g) Dimpled TT 25 mm inserted tubes at the lateral cross-section plain for Re=20000.

In Figure 4.9., streamlines through the tubes can be seen. As it is similar to Figure 4.8, streamlines show the velocity values in the tube. While perforations don't seem to affect the flow, dimples especially with lower distances cause higher disturbances in the flow. Hence, it is expected that this phenomenon cause thermal boundary layer mixing and higher thermal performances, consequently more homogeneous temperature distribution across the tube surface as seen in Figure 4.10. This is also seen in Figure 4.11, surface temperature contours of twisted tapes and in Figure 4.12, temperature contours at the lateral cross-section plain of the tubes. Smooth twisted tape presents lower Nusselt number and due to that, temperature gradiant is higher compared to others. On the other hand, dimpled twisted tapes have lower average temperature gradients.

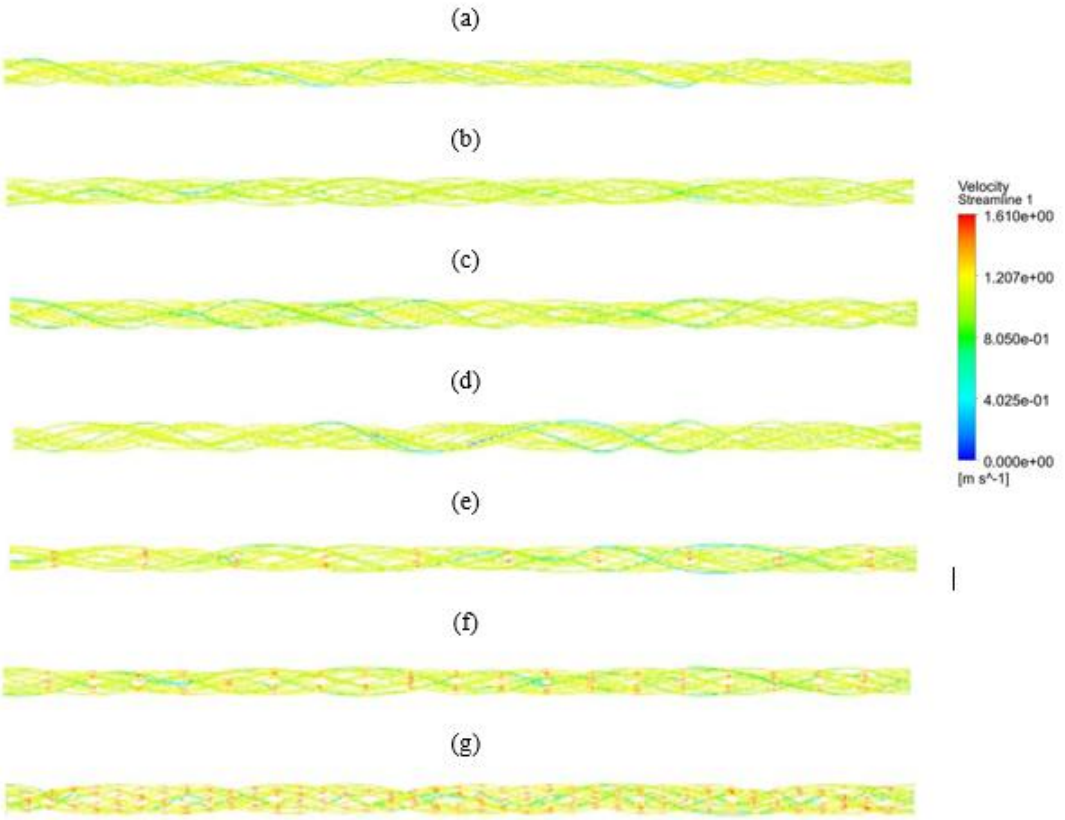

Figure 4.9. Velocity streamlines throughout a) Plain TT, b) Perforated TT 100 mm, c) Perforated TT 50 mm, d) Perforated TT 25 mm, e) Dimpled TT 100 mm, f) Dimpled TT 50 mm, g) Dimpled TT 25 mm inserted tubes for Re=20000.

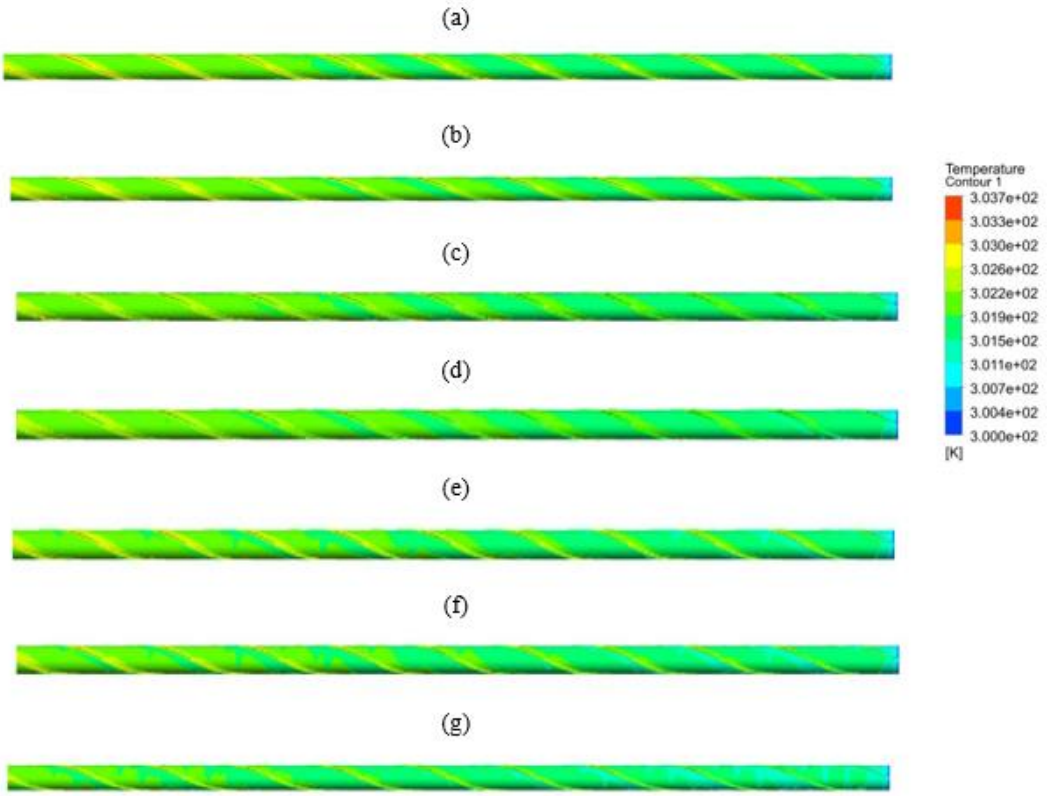

Figure 4.10. Wall surface temperature contours of a) Plain TT, b) Perforated TT 100 mm, c) Perforated TT 50 mm, d) Perforated TT 25 mm, e) Dimpled TT 100 mm, f) Dimpled TT 50 mm, g) Dimpled TT 25 mm inserted tubes for Re=20000.

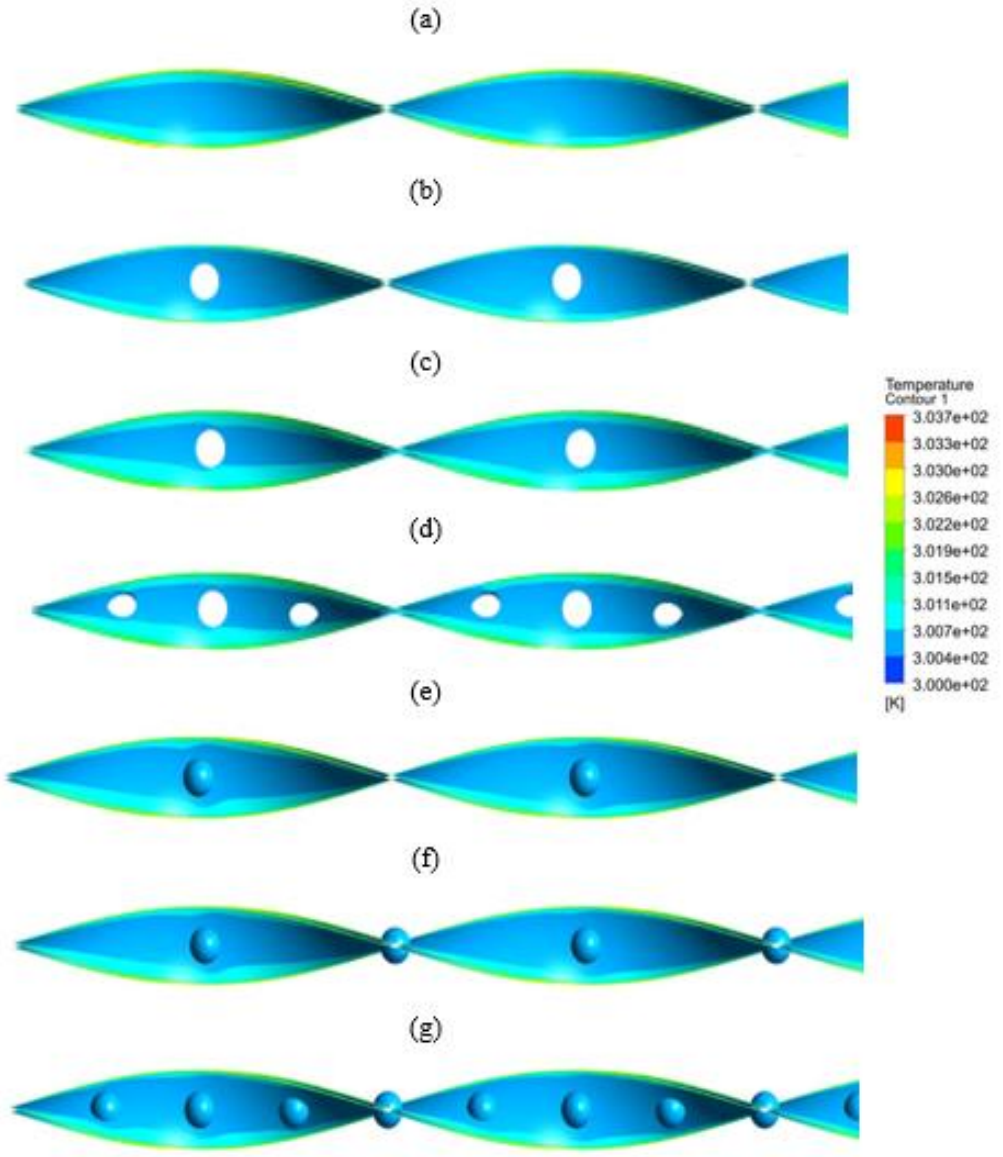

Figure 4.11. Twisted tape surface temperature contours of a) Plain TT, b) Perforated TT 100 mm, c) Perforated TT 50 mm, d) Perforated TT 25 mm, e) Dimpled TT 100 mm, f) Dimpled TT 50 mm, g) Dimpled TT 25 mm inserted tubes for Re=20000.

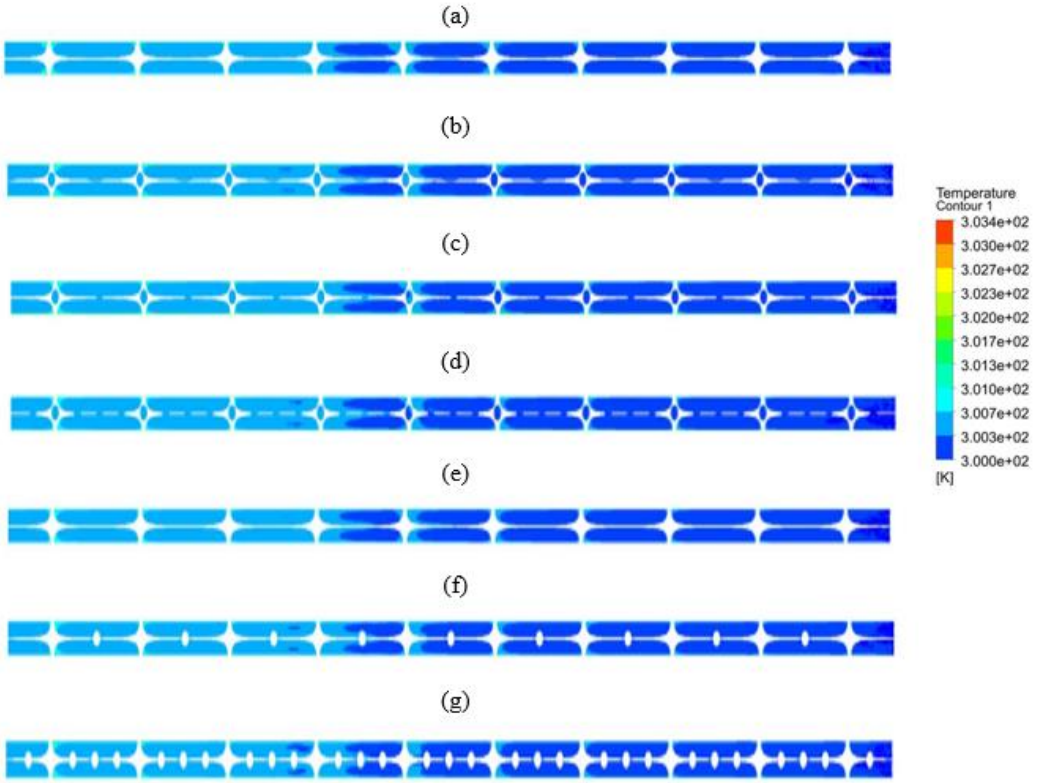

Figure 4.12. Temperature contours of a) Plain TT, b) Perforated TT 100 mm, c) Perforated TT 50 mm, d) Perforated TT 25 mm, e) Dimpled TT 100 mm, f) Dimpled TT 50 mm, g) Dimpled TT 25 mm inserted tubes at the lateral cross-section plain for Re=20000.

Figure 4.13 and 4.14 shows the turbulence kinetic energy at the lateral cross-section plain of the tubes. Turbulence kinetic energy is clear indicator for eddies in turbulent flows, so the effect of perforations and dimples on the flow is seen in the figures. Dimples contribute to turbulence kinetic energy more than perforations, because dimple fins disturb the flow more easily. Hence, it can be reached that eddies caused by the perforations and dimples provide higher heat transfer rates.

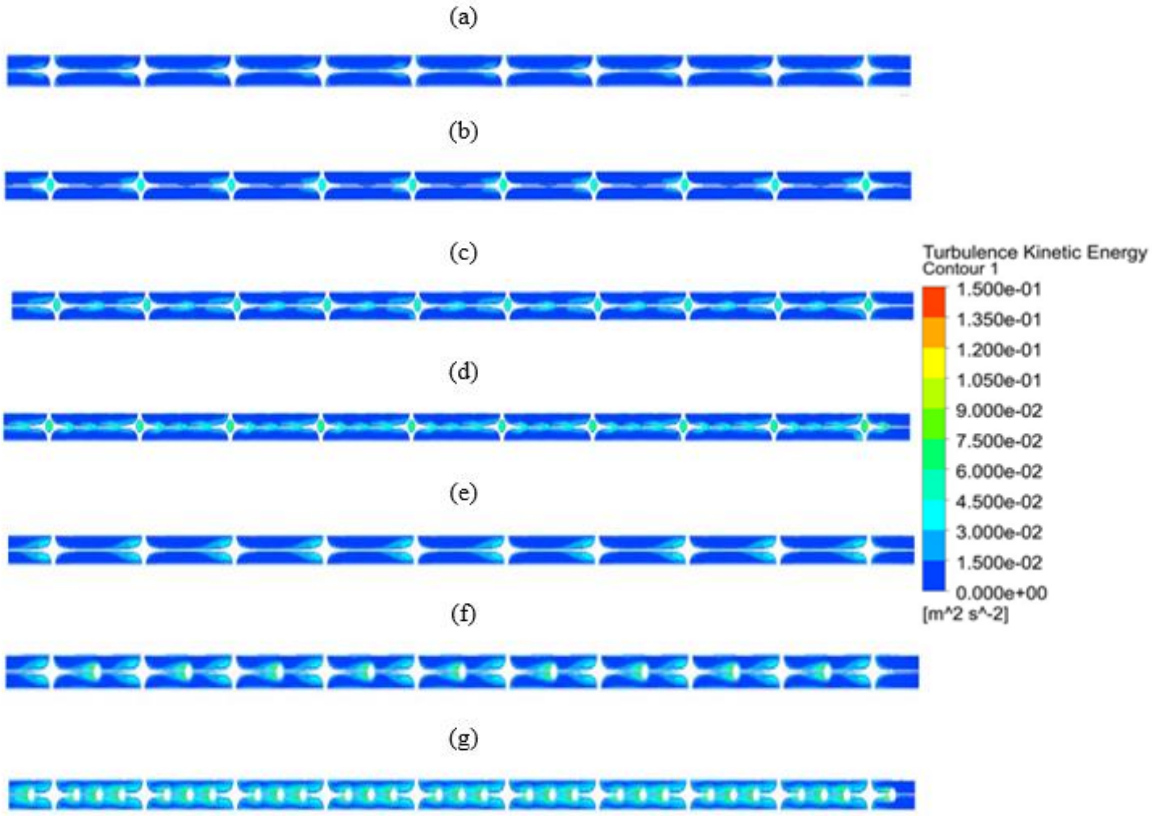

Figure 4.13. Turbulence kinetic energy contours of a) Plain TT, b) Perforated TT 100 mm, c) Perforated TT 50 mm, d) Perforated TT 25 mm, e) Dimpled TT 100 mm, f) Dimpled TT 50 mm, g) Dimpled TT 25 mm inserted tubes at the lateral cross-section plain for Re=20000.

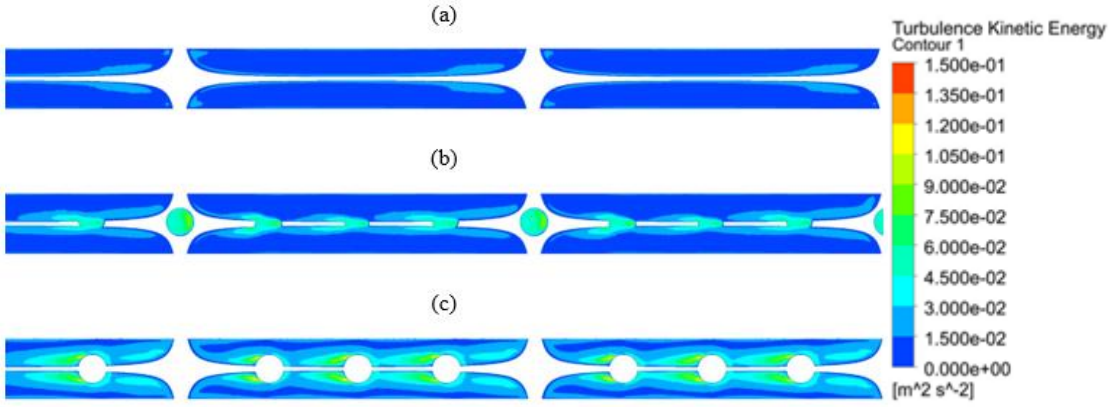

Figure 4.14. Detailed turbulence kinetic energy contours of a) Plain TT, b) Perforated TT 25 mm, c) Dimpled TT 25 mm inserted tubes at the lateral cross-section plain for Re=20000.

PART 5

CONCLUSION

After reviewing and discussing the results that is obtained from the previous seven cases and comparing them to the smooth tube, following outcomes have been reached.

- The highest Nusselt number for heat transfer was obtained in the case of 25 mm dimpled twisted tape at all Reynolds numbers when compared with the other cases.
- The best improvement was obtained for the dimpled twisted tape 25mm where it 42 % while the perforated tapes was 28.7% and the plain tape was 24%.
- The addition of the dimples to the twisted tape was useful in improving the Nusselt number, especially when increasing the number of dimples in the twisted tape.
- Note that the lowest Nusselt value was obtained at smooth tube.
- Increasing the number of dimpled and perforated it causes to high pressure leads to an increase in the value of the friction factor.
- The highest value of fraction factors at dimpled twisted tape 25 mm.
- The lowest PEC was obtained with dimpled twisted tape 25mm because to increase in the friction factor which is inversely proportional to the PEC.

REFERENCES

1. Bucak, H., & Yilmaz, F., "Heat transfer augmentation using periodically spherical dimple-protrusion patterned walls of twisted tape," **International Journal of Thermal Sciences**, 171, 107211, (2022).

2. Mogra, A., Pandey, P. K., and Gupta, K. K., "Enhancement of boiling heat transfer performance using nano coating-A review", **Journal Of Advanced Research In Fluid Mechanics And Thermal Sciences**, 71 (1): 100–116 (2020).

3. Liu, H., Zheng, G., Man, C., Jiang, K., & Lv, X., "Numerical and Experimental Studies on Heat Transfer Enhancement in a Circular Tube Inserted with Twisted Tape Inserts," **American Journal of Energy Engineering**, 9(2), 30-40, (2021).

4. Hong, Y., Du, J., & Wang, S., "Experimental heat transfer and flow characteristics in a spiral grooved tube with overlapped large/small twin twisted tapes," **International Journal of Heat and Mass Transfer**, 106, 1178-1190, (2017).
5. Bhuiya, M. M. K., Chowdhury, M. S. U., Saha, M., & Islam, M. T., "Heat transfer and friction factor characteristics in turbulent flow through a tube fitted with perforated twisted tape inserts," **International Communications in Heat and Mass Transfer**, 46, 49-57, (2013).

6. C., R. B., Kumar, P., Roy, S., and Ganesan, R., "A comprehensive review on compound heat transfer enhancement using passive techniques in a heat exchanger", **Materials Today: Proceedings**, 54: 428–436 (2022).

7. Thapa, S., Samir, S., Kumar, K., and Singh, S., "A review study on the active methods of heat transfer enhancement in heat exchangers using electroactive and magnetic materials", **Materials Today: Proceedings**, 45: 4942–4947 (2021).

8. Akhavan-Behabadi, M. A., Kumar, R., Mohammadpour, A., and Jamali-Asthiani, M., "Effect of twisted tape insert on heat transfer and pressure drop in horizontal evaporators for the flow of R-134a", **International Journal Of Refrigeration**, 32 (5): 922–930 (2009).

9. Liao, Q. and Xin, M. D., "Augmentation of convective heat transfer inside tubes with three-dimensional internal extended surfaces and twisted-tape inserts", **Chemical Engineering Journal**, 78 (2–3): 95–105 (2000).

10. Khargotra, R., Kumar, R., Nadda, R., Dhingra, S., Alam, T., Dobrota, D., Chicea, A. L., András, K., and Singh, T., "A review of different twisted tape configurations used in heat exchanger and their impact on thermal performance of the system", **Heliyon**, 9 (6): e16390 (2023).

11. Oni, T. O., & Paul, M. C., "Numerical investigation of heat transfer and fluid flow of water through a circular tube induced with divers' tape inserts," **Applied Thermal Engineering**, 98, 157-168, (2016).

12. Saysroy, A., & Eiamsa-Ard, S., "Enhancing convective heat transfer in laminar and turbulent flow regions using multi-channel twisted tape inserts," **International Journal of Thermal Sciences**, 121, 55-74, (2017).

13. Liu, X., Li, C., Cao, X., Yan, C., & Ding, M., "Numerical analysis on enhanced performance of new coaxial cross twisted tapes for laminar convective heat transfer," **International Journal of Heat and Mass Transfer**, 121, 1125-1136, (2018).

14. Eiamsa-ard, S., Thianpong, C., & Eiamsa-ard, P., "Turbulent heat transfer enhancement by counter/co-swirling flow in a tube fitted with twin twisted tapes," **Experimental Thermal and Fluid Science**, 34(1), 53-62, (2010).

15. Kumbhar, D. G., & Sane, N. K., "Heat transfer enhancement in a circular tube twisted with swirl generator: A review," **Proc. of the 3rd International Conference on Advances In Mechanical Engineering**, (2010).

16. Lunsford, K. M., "Increasing heat exchanger performance," **Hydrocarbon engineering**, 77, 786-793, (1998).

17. Dewan, A., Mahanta, P., Raju, K. S., & Kumar, P. S., "Review of passive heat transfer augmentation techniques," **Proceedings of the Institution of Mechanical Engineers, Part A: Journal of Power and Energy**, 218(7), 509-527, (2004).

18. Kraus, A. D., "Process, enhanced, and multiphase heat transfer," **Begell House**, (1996).

19. Bergles, A. E., "The implications and challenges of enhanced heat transfer for the chemical process industries," **Chemical Engineering Research and Design**, 79(4), 437-444, (2001).

20. Dagdevir, T., & Ozceyhan, V., "An experimental study on heat transfer enhancement and flow characteristics of a tube with plain, perforated and dimpled twisted tape inserts," **International Journal of Thermal Sciences**, 159, 106564, (2021).

21. Tusar, M., Ahmed, K., Bhuiya, M., Bhowmik, P., Rasul, M., & Ashwath, N., "CFD study of heat transfer enhancement and fluid flow characteristics of laminar flow through tube with helical screw tape insert," **Energy Procedia**, 160, 699-706, (2019).

22. Liaw, K. L., Kurnia, J. C., & Sasmito, A. P., "Turbulent convective heat transfer in helical tube with twisted tape insert," **International Journal of Heat and Mass Transfer**, 169, 120918, (2021).

23. Ravikiran, B., Ramji, K., & Subrahmanyam, T., "Investigation on thermal performance of different wire coil twisted tape inserts in a tube circulated with water," **International Communications in Heat and Mass Transfer**, 122, 105148, (2021).

24. He, W., Toghraie, D., Lotfipour, A., Pourfattah, F., Karimipour, A., & Afrand, M., "Effect of twisted-tape inserts and nanofluid on flow field and heat transfer characteristics in a tube," **International Communications in Heat and Mass Transfer**, 110, 104440, (2020).

25. Ju, Y., Zhu, T., Mashayekhi, R., Mohammed, H. I., Khan, A., Talebizadehsardari, P., Yaïci, W., "Evaluation of multiple semi-twisted tape inserts in a heat exchanger pipe using Al2O3 nanofluid," **Nanomaterials**, 11(6), 1570, (2021).

26. Paneliya, S., Prajapati, P., Patel, U., Trivedi, I., Patel, A., Patel, K., & Khanna, S., "Experimental and CFD analysis on heat transfer and fluid flow characteristic of a tube equipped with variable pitch twisted tape," **E3S Web of Conferences**, 116, 00058, (2019).

27. Salman, S. D., Kadhum, A. A. H., Takriff, M. S., & Mohamad, A. B., "Heat transfer enhancement of laminar nanofluids flow in a circular tube fitted with parabolic-cut twisted tape inserts," **The Scientific World Journal**, (2014).

28. Yadav, R. J., & Padalkar, A. S., "CFD analysis for heat transfer enhancement inside a circular tube with half-length upstream and half-length downstream twisted tape," **Journal of Thermodynamics**, (2012).

29. Mokkapati, V., & Lin, C. S., "Numerical study of an exhaust heat recovery system using corrugated tube heat exchanger with twisted tape inserts," **International Communications in Heat and Mass Transfer**, 57, 53-64, (2014).

30. Liu, H., Zheng, G., Man, C., Jiang, K., & Lv, X., "Numerical and Experimental Studies on Heat Transfer Enhancement in a Circular Tube Inserted with Twisted Tape Inserts," **American Journal of Energy Engineering**, 9(2), 30-40, (2021).

31. Kumar, B., Kumar, M., Patil, A. K., & Jain, S., "Effect of V cut in perforated twisted tape insert on heat transfer and fluid flow behavior of tube flow: an experimental study," **Experimental Heat Transfer**, 32(6), 524-544, (2019).

32. Sivasubramanian, M., Jaganathan, K. D., "Experimental investigations to study the influence of twisted tape insert on heat transfer equipment – an extensive review," **Journal of Critical Reviews**, 7 (14), 768-777, (2020).

33. Bhuiya, M. M. K., Azad, A. K., Chowdhury, M. S. U., & Saha, M., "Heat transfer augmentation in a circular tube with perforated double counter twisted tape inserts," **International Communications in Heat and Mass Transfer**, 74, 18-26, (2016).

34. Faridi Khouzestani, R., & Ghafouri, A., "Numerical study on heat transfer and nanofluid flow in pipes fitted with different dimpled spiral center plate," **SN Applied Sciences**, 2(2), 298, (2020).

35. Guo, J., Fan, A., Zhang, X., & Liu, W., "A numerical study on heat transfer and friction factor characteristics of laminar flow in a circular tube fitted with center-cleared twisted tape," **International Journal of Thermal Sciences**, 50(7), 1263-1270, (2011).

36. Kumar, S., Dinesha, P., Narayanan, A., & Nanda, R., "Numerical investigation on the heat transfer characteristics in a circular pipe using multiple twisted tapes in laminar flow conditions," **Heat Transfer—Asian Research**, 48(7), 3399-3419, (2019).

37. Safikhani, H., & Abbasi, F., "Numerical study of nanofluid flow in flat tubes fitted with multiple twisted tapes," **Advanced Powder Technology**, 26(6), 1609-1617, (2015).

38. Zheng, L., Xie, Y., & Zhang, D., "Numerical investigation on heat transfer performance and flow characteristics in circular tubes with dimpled twisted tapes using Al2O3-water nanofluid," **International Journal of Heat and Mass Transfer**, 111, 962-981, (2017).

39. Thianpong, C., Eiamsa-Ard, P., Wongcharee, K., & Eiamsa-Ard, S., "Compound heat transfer enhancement of a dimpled tube with a twisted tape swirl generator," **International communications in heat and mass transfer**, 36(7), 698-704, (2009).

40. Nakhchi, M. E., & Esfahani, J. A., "Numerical investigation of rectangular-cut twisted tape insert on performance improvement of heat exchangers," **International Journal of Thermal Sciences**, 138, 75-83, (2019).

41. Al-Obaidi, A. R., "Investigation of the flow, pressure drop characteristics, and augmentation of heat performance in a 3D flow pipe based on different inserts of twisted tape configurations," **Heat Transfer**, 50(5), 5049-5079, (2021).

42. Bhattacharyya, S., Chattopadhyay, H., & Benim, A. C., "Simulation of heat transfer enhancement in tube flow with twisted tape insert," **Progress in Computational Fluid Dynamics, an International Journal**, 17(3), 193-197, (2017).

43. Hong, Y., Du, J., & Wang, S., "Experimental heat transfer and flow characteristics in a spiral grooved tube with overlapped large/small twin twisted tapes," **International Journal of Heat and Mass Transfer**, 106, 1178-1190, (2017).

44. Dagdevir, T., Uyanik, M., & Ozceyhan, V., "The experimental thermal and hydraulic performance analyses for the location of perforations and dimples on the twisted tapes in twisted tape inserted tube," **International Journal of Thermal Sciences**, 167, 107033, (2021).

45. Thianpong, C., Eiamsa-Ard, P., Promvonge, P., & Eiamsa-Ard, S., "Effect of perforated twisted-tapes with parallel wings on heat tansfer enhancement in a heat exchanger tube," **Energy procedia**, 14, 1117-1123, (2012).

46. Nakhchi, M. E., Hatami, M., & Rahmati, M., "Experimental investigation of heat transfer enhancement of a heat exchanger tube equipped with double-cut twisted tapes," **Applied Thermal Engineering**, 180, 115863, (2020).

47. Mushatet, K. S., Rishak, Q. A., & Fagr, M. H., "Experimental and numerical investigation of swirling turbulent flow and heat transfer due to insertion of twisted tapes of new models in a heated tube," **Applied Thermal Engineering**, 171, 115070, (2020).

48. Bucak, H., & Yilmaz, F., "Heat transfer augmentation using periodically spherical dimple-protrusion patterned walls of twisted tape," **International Journal of Thermal Sciences**, 171, 107211, (2022).

49. Bhuiya, M. M. K., Roshid, M. M., Talukder, M. M. M., Rasul, M. G., & Das, P., "Influence of perforated triple twisted tape on thermal performance characteristics of a tube heat exchanger," **Applied Thermal Engineering**, 167, 114769, (2020).

50. Nanan, K., Thianpong, C., Promvonge, P., & Eiamsa-Ard, S., "Investigation of heat transfer enhancement by perforated helical twisted-tapes," **International Communications in Heat and Mass Transfer**, 52, 106-112, (2014).

51. Bhuiya, M. M. K., Chowdhury, M. S. U., Saha, M., & Islam, M. T., "Heat transfer and friction factor characteristics in turbulent flow through a tube fitted with perforated twisted tape inserts," **International Communications in Heat and Mass Transfer**, 46, 49-57, (2013).

52. Hasanpour, A., Farhadi, M., & Sedighi, K., "Experimental heat transfer and pressure drop study on typical, perforated, V-cut and U-cut twisted tapes in a helically corrugated heat exchanger," **International Communications in Heat and Mass Transfer**, 71, 126-136, (2016).

53. Nakhchi, M. E., & Esfahani, J. A., "Numerical investigation of turbulent CuO–water nanofluid inside heat exchanger enhanced with double V-cut twisted tapes," **Journal of Thermal Analysis and Calorimetry**, 145, 2535-2545, (2021).

54. Khalil, A., Elshenawy, E. A., El-Samadony, Y. A. F., & Salem, A. M., "NUMERICAL STUDY OF ENHANCING HEAT TRANSFER USING TWISTED TAPE INSERTS," **ERJ. Engineering Research Journal**, 36(4), 441-455, (2013).

55. Dhumal, A. H., Kerkal, G. M., & Pawale, K. T., "Heat transfer enhancement for tube in tube heat exchanger using twisted tape inserts," **International Journal of Advanced Engineering Research and Science**, 4(5), 237166, (2017).

56. Feizabadi, A., Khoshvaght-Aliabadi, M., & Rahimi, A. B., "Experimental evaluation of thermal performance and entropy generation inside a twisted U-tube equipped with twisted-tape inserts," **International Journal of Thermal Sciences**, 145, 106051, (2019).

57. Bhattacharyya, S., Benim, A. C., Chattopadhyay, H., & Banerjee, A., "Experimental investigation of heat transfer performance of corrugated tube with spring tape inserts," **Experimental Heat Transfer**, 32(5), 411-425, (2019).

58. Sarada, S. N., Sita, A. V, Raju, R., Kalyani Radha, K., and Shyam Sunder, L., "Enhancement of heat transfer using varying width twisted tape inserts", **International Journal Of Engineering, Science And Technology**, 2 (6): 107–118 (2010).

59. Liang, Y., Liu, P., Zheng, N., Shan, F., Liu, Z., and Liu, W., "Numerical investigation of heat transfer and flow characteristics of laminar flow in a tube with center-tapered wavy-tape insert", **Applied Thermal Engineering**, 148: 557–567 (2019).

60. Mohammed, A. A. and Mohammed, A., "Heat Transfer Augmentation in Tube Fitted with Rotating Twisted Tape Insert An investigation into mixed convectionheat transfer in an inclined annuli View project Heat Transfer View

project", **Journal of Mechanical Engineering Research and Developments**, 43:308-316 (2020).

61. Humam Kareem Jalghaf, "Numerical and Experimental Investigation of Heat Transfer Enhancement in Slot Groove Circular Tube with Internal Twisted Tape". **Al-Nahrain Journal for Engineering Sciences**, 20:1228-1239 (2017).

62. Yan He et, " Experimental study on Heat transfer enhancement characteristics of the tube with cross hollow twisted tape inserts " **Applied Thermal Engineering**, 12:.029 (2017).

63. Sørensen, L. S., "An introduction to computational fluid dynamics: the finite volume method," (1999).

64. Cengel, Y. A., "Heat transfer: a practical approach," (1998).

65. Feynman, R. P., Leighton, R. B., Sands, M., "The feynman lectures on physics; vol. I," **American Journal of Physics**, 33(9), 750-752, (1965).

66. Hagengruber, R., "Émilie du Châtelet between Leibniz and Newton: the transformation of Metaphysics," In Emilie du Châtelet between Leibniz and Newton (pp. 1-59). **Dordrecht: Springer Netherlands**, (2011).

67. Arianrhod, R., "Seduced by logic: Émilie du Châtelet, Mary Somerville and the Newtonian revolution," **Oxford University Press**, USA, (2012).

68. Planck, M., "Treatise on Thermodynamics, third English edition translated by A. Ogg from the seventh German edition," **Longmans, Green & Co**, London, UK.

69. Witten, E., "A new proof of the positive energy theorem," **Communications in Mathematical Physics**, 80(3), 381-402, (1981).

70. Handbook, A. S. H. R. A. E., "ASHRAE Handbook-Fundamental: SI Editions," **American society of heating, refrigerating and air-conditioning engineers. Inc**.: Atlanta, GA, USA, (2009).

71. Coulson, J. M., "Coulson & Richardson Chemical Engineering, Volume 1," disp, 10, 32, (2000).

RESUME

The researcher was graduated from the Mechanical Engineering Department, University of Technology Baghdad in 29/7/2003 for the academic year 2002/2003. He joined the master study in Karabuk University 23/9/2020.